Appendix A.22:

31 Landy St – CPT 44439 (VsVp 57203)

Table 1: Site Description for 31 Landy St (CPT 44439 – VsVp 57322).

Attribute	Yes/No			Description/Date	Symbol in Figure 1
	10-m Buffer	20-m Buffer	50-m Buffer		
Near a body of surface water or other free face features?	No	No	No	The center of the site is ~250 m to the NW and ~330 m to the N from the Avon River (the free-face height is ~1.5-2 m).	NA
Lateral spreading observed during the CES?	No	No	No	Lateral spreading was not observed by the observed by the mapping team.[1] Ground cracks <50mm in width in the W portion of all buffers are likely oscillation cracks.	NA
Nearby buildings or structures?	Yes	Yes	Yes	Building coverage of the 10-, 20-, and 50-m buffers is 41, 31, and 25%, respectively. Buildings are in all quadrants of all buffers.	White Fill + Brown Outline
Sloping land?	No	No	No	Flat land, residential area	NA
Step changes in the ground surface?	No	No	No	NA	NA
Retaining walls?	No	No	No	NA	NA
Vegetation?	Yes	Yes	Yes	Trees and bushes cover 22, 22, and 20% of the 10-, 20-, and 50-m buffers, respectively. They are in the E portion of the 10-m buffer and all quadrants of the 20-m and 50-m buffers.	White Fill + Green Outline
Anthropogenic changes to the site between the LiDAR surveys?	Yes	Yes	Yes	Road construction in the NW q. of the 50-m b. between Apr 2012 and Oct 2012. New road in the NW q. of the 50-m b. in Mar 2013. Building removal in the SE q. of the 50-m b. between Mar 2013 and Aug 2013. Swimming pool removal in the SE q. of the 20- and 50-m b. between Aug 2013 and Feb 2014. Building removal in the NW q. of all b. and vegetation removal in the NW q. of the 50-m b. between Feb 2014 and Mar 2014. Building removal in the SW q. of the 50-m b., the W portion of all b., and the SE q. of the 50-m b. between Mar 2014 and Aug 2014. Building removal in the SW q. of the 50-m b. and the SE q. of the 50-m b. between Aug 2014 and Sep 2014. Building removal in the E portion of the 50-m b. between June 2015 and July 2015 and building addition at the same property between July 2015 and Sep 2015.	Building Addition/ Removal: Orange Crossline; Vegetation Removal: Green Crossline
Other important factors?	No	Yes	Yes	Low-motor-vehicle-volume road (Landy St) occupies 7% of the 50-m buffer and stretches throughout the NE and NW quadrants. The swimming pool in the SE quadrant of the 20- and 50-m buffers remained filled with ejecta from the Feb 2011 EQ until its removal between Aug 2013 and Feb 2014.	Swimming Pool: White Fill + Blue Outline

Note: Buffer is the area within a circle of a specified radius with CPT investigations done at its center (172.678436°, -43.514681°).

[1] Canterbury Geotechnical Database. (2012). "Observed Ground Crack Locations", Map Layer CGD0400 - 23 July 2012, retrieved July 09, 2018 from https://canterburygeotechnicaldatabase.projectorbit.com/

Figure 1: Site plan with areas where ejecta-induced settlement is considered.

Note 1: Two patches (outlined in red) in the free field were selected for settlement assessment as areas free of vegetation and structures. Other important factors considered for the patch selection were its proximity to a CPT, a property subjected to addition and/or demolition of a structure, front yard/backyard alterations (e.g., ploughing, rubble, scrap), and aerial distribution of sediment ejecta. In addition, the entire portion of the road within the 50-m buffer was considered for settlement assessment. Roads as hard, relatively flat surfaces provide many ground-classified points. The LiDAR-based settlement analyses of Patch A were not conducted for any earthquake event due to the evident absence of ejecta. The Oct 2015 LiDAR was not used in the settlement analysis of the Road due to the anthropogenic changes after Apr 2012. The ejecta inside the swimming pool was estimated for the Feb-11 EQ using the physical evidence only.

Table 2: LiDAR flight error adjustments, global adjustments for the difference between average LiDAR point elevations and benchmark survey elevations, and vertical tectonic movement adjustments.

	Adjustments (mm)		
Earthquake Event(s)	LiDAR Flight Error	Global Offset[2]	Tectonic Vertical Movement
Sep-10	0	-3	0
Feb-11	0	16	-50
Jun-11	0	38	-45
Dec-11	-50	-65	0
CES	-50	-14	-95
Any LiDAR survey affected by ejecta?			Yes*

Note: The negative sign indicates the subtraction from the ground surface subsidence, while the positive sign indicates the addition to the ground surface subsidence; * indicates that ejecta were present on the Road and within Patch B at the time of the Sep-10 LiDAR survey and some ejecta remained on the Road and within Patch B during the Mar 2011 LiDAR survey and potentially May 2011 LiDAR survey (thus add ~30 mm to the ground surface subsidence for the Sep-10 EQ and subtract ~30 mm from the ground surface subsidence for the Jun-11 EQ).

Table 3a: LiDAR Measurement Error for Patch B.

Surveys	Buffer	Area Averaged Difference Indicating Repeat Measurement Error (mm)	$\sigma^*_{\text{individual LiDAR points}}$ (mm)	%Reduction in σ due to Area Averaging of LiDAR Points
Post Feb 2011: Mar 2011 and May 2011	10-m	NA	59	[37,37]
	20-m	NA		
	50-m	22		
Post Dec 2011: Feb 2012 and Oct 2015	10-m	NA	70	[9,9]
	20-m	NA		
	50-m	6		

*Standard deviation.

[2] Russell, J., & van Ballegooy, S. (2015). *Canterbury Earthquake Sequence: Increased liquefaction vulnerability assessment methodology*. New Zealand: Tonkin & Taylor Ltd.

Table 3b: LiDAR Measurement Error for Road.

Surveys	Buffer	Area Averaged Difference Indicating Repeat Measurement Error (mm)	$\sigma^*_{\text{individual LiDAR points}}$ (mm)	%Reduction in σ due to Area Averaging of LiDAR Points
Post Feb 2011: Mar 2011 and May 2011	10-m	NA	59	[49,49]
	20-m	NA		
	50-m	29		
Post Dec 2011: Feb 2012 and Oct 2015	10-m	NA	70	[ND,ND]
	20-m	NA		
	50-m	ND		

*Standard deviation; ND = Not determined.

Table 4a: Ground surface subsidence adjustments due to LiDAR measurement error for Patch B.

Earthquake Event(s)	$\sigma_{\text{pre-EQ LiDAR survey}}$ (mm)	$\sigma_{\text{post-EQ LiDAR survey}}$ (mm)	σ_{total} (mm)	Area Average Adjusted σ (mm) **
Sep-10	158	56	134	±50
Feb-11	56	59	59	±22
Jun-11	59	61	62	±23
Dec-11	61	70	87	±32
CES	158	70	124	±46

**Based on the highest %Reduction in Table 3a.

Table 4b: Ground surface subsidence adjustments due to LiDAR measurement error for Road.

Earthquake Event(s)	$\sigma_{\text{pre-EQ LiDAR survey}}$ (mm)	$\sigma_{\text{post-EQ LiDAR survey}}$ (mm)	σ_{total} (mm)	Area Average Adjusted σ (mm) **
Sep-10	158	56	134	±66
Feb-11	56	59	59	±29
Jun-11	59	61	62	±31
Dec-11	61	70	87	±43
CES	158	70	124	±61

**Based on the highest %Reduction in Table 3b.

Table 5a: Raw liquefaction-related ground surface subsidence using original LiDAR points for Patch B.

	Average Ground Surface Subsidence (mm)		
Earthquake Event(s)	10-m Buffer	20-m Buffer	50-m Buffer
Sep-10	NA	NA	-17
Feb-11	NA	NA	197
Jun-11	NA	NA	59
Dec-11	NA	NA	64
CES	NA	NA	303

Table 5c: Raw liquefaction-related ground surface subsidence using original LiDAR points for Road.

	Average Ground Surface Subsidence (mm)		
Earthquake Event(s)	10-m Buffer	20-m Buffer	50-m Buffer
Sep-10	NA	NA	-31
Feb-11	NA	NA	191
Jun-11	NA	NA	60
Dec-11	NA	NA	95
CES	NA	NA	315

Table 6a: Corrected liquefaction-related ground surface subsidence using original LiDAR points for Patch B with the calculated adjustments in Table 2.

	Average Calculated Ground Surface Subsidence (mm)		
Earthquake Event(s)	10-m Buffer	20-m Buffer	50-m Buffer
Sep-10	NA	NA	10±50
Feb-11	NA	NA	163±25
Jun-11	NA	NA	22±25
Dec-11	NA	NA	-51±25
CES	NA	NA	144±50

Notes: Plus/minus values are same as those in Table 4a, but rounded to the nearest 25; Positive overall values indicate ground surface subsidence, while negative overall values indicate ground surface uplift.

Table 6b: Corrected liquefaction-related ground surface subsidence using original LiDAR points for Road with the calculated adjustments in Table 2.

	Average Calculated Ground Surface Subsidence (mm)		
Earthquake Event(s)	10-m Buffer	20-m Buffer	50-m Buffer
Sep-10	NA	NA	-4±75
Feb-11	NA	NA	157±25
Jun-11	NA	NA	23±25
Dec-11	NA	NA	-20±50
CES	NA	NA	156±50

Notes: Plus/minus values are same as those in Table 4c, but rounded to the nearest 25; Positive overall values indicate ground surface subsidence, while negative overall values indicate ground surface uplift.

Table 7a: Corrected liquefaction-related ground surface subsidence for Patch B using LiDAR DEMs.

	Estimated Ground Surface Subsidence (mm)								
	10-m Buffer			20-m Buffer			50-m Buffer		
Earthquake Event(s)	16th %ile	50th %ile	84th %ile	16th %ile	50th %ile	84th %ile	16th %ile	50th %ile	84th %ile
Sep-10	NA	NA	NA	NA	NA	NA	-50	-50	50
Feb-11	NA	NA	NA	NA	NA	NA	150	150	150
Jun-11	NA	NA	NA	NA	NA	NA	<50	50	50
Dec-11	NA	NA	NA	NA	NA	NA	<50	<50	<50
CES	NA	NA	NA	NA	NA	NA	200	200	200

Note: These percentiles are not the exact statistical measures; they indicate the spatial variability of ground surface subsidence.

Table 7b: Corrected liquefaction-related ground surface subsidence for Road using LiDAR DEMs.

	Estimated Ground Surface Subsidence (mm)								
	10-m Buffer			20-m Buffer			50-m Buffer		
Earthquake Event(s)	16th %ile	50th %ile	84th %ile	16th %ile	50th %ile	84th %ile	16th %ile	50th %ile	84th %ile
Sep-10	NA	NA	NA	NA	NA	NA	50	50	100
Feb-11	NA	NA	NA	NA	NA	NA	100	150	150
Jun-11	NA	NA	NA	NA	NA	NA	<50	50	50
Dec-11	NA	NA	NA	NA	NA	NA	<50	<50	<50
CES	NA	NA	NA	NA	NA	NA	200	200	200

Note: These percentiles are not the exact statistical measures; they indicate the spatial variability of ground surface subsidence.

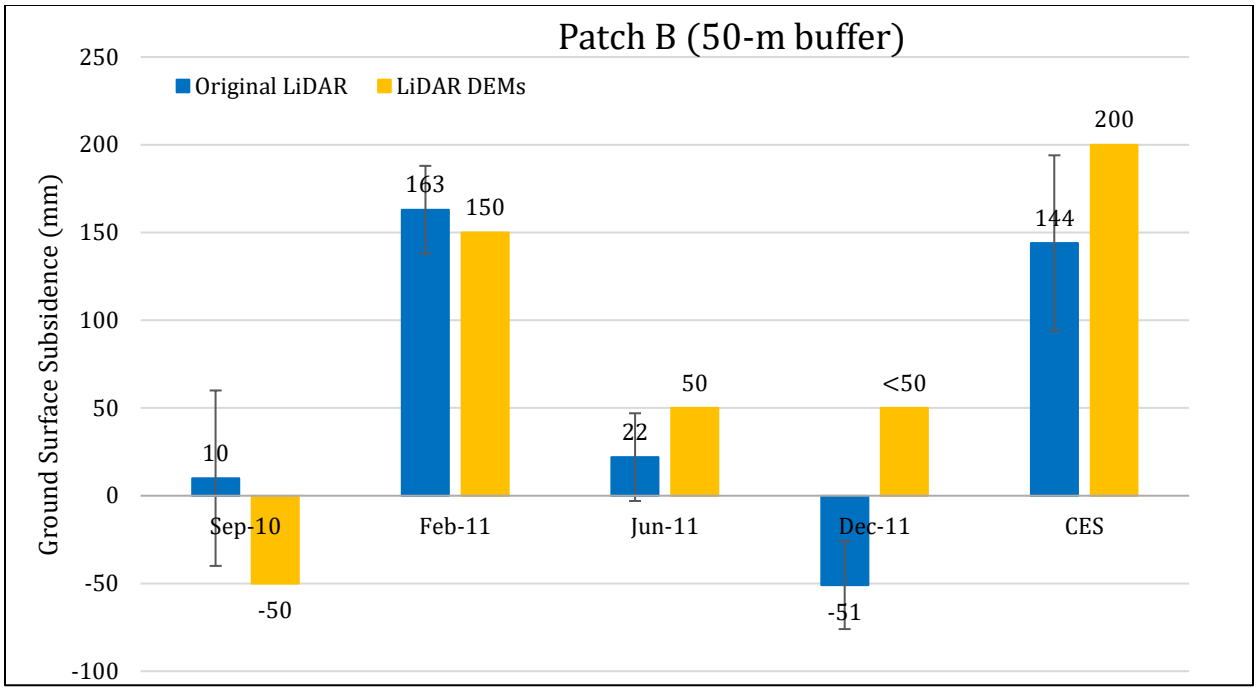

Figure 2: Comparison between ground surface subsidence determined from original LiDAR survey points and ground surface subsidence (50th %ile) estimated using LiDAR DEMs for Patch B.

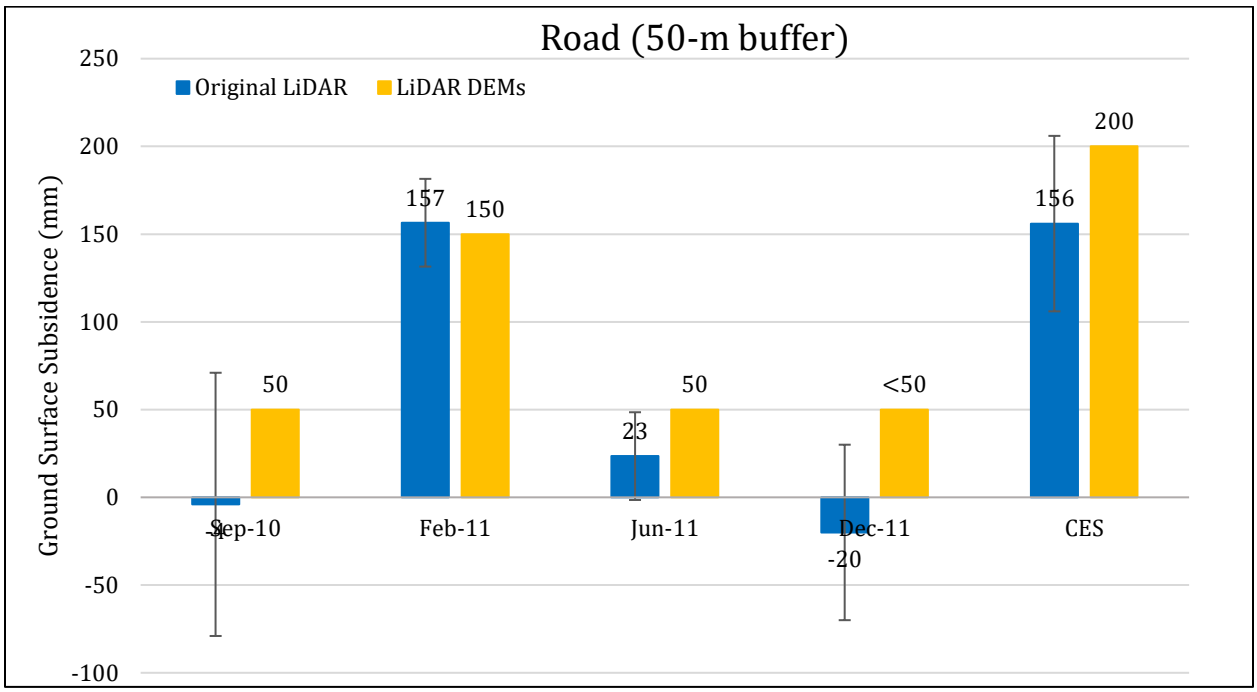

Figure 3: Comparison between ground surface subsidence determined from original LiDAR survey points and ground surface subsidence (50th %ile) estimated using LiDAR DEMs for Road (50-m buffer).

Note 2: The ground surface subsidence values determined from the original LiDAR survey points are generally consistent with the ground surface subsidence values estimated using the LiDAR DEMs for all earthquake events. The ground surface uplift observed for Patch B (LiDAR DEM) for the Sep-10 EQ may be due to the limited number of the July 2003 elevation points and the DEM cell interpolation.

Table 8a: Ejecta-Induced settlement for the top 20 m of the soil profile for Patch A for the 50th %ile PGA, P_L=50%, and C_{FC}=0.13 using BI-2014, ZRB-2002, and I_c cutoff of 2.6.

Earthquake Event(s)	M_W	PGA (g)	Depth to Groundwater (m)	S_T (mm)	S_{V1D} (mm)	$S_{E,L}$ (mm)
Sep-10	7.1	0.20	1.5	ND	25±20	ND
Feb-11	6.2	0.45	1.5	ND	130±50	ND
Jun-11	6.2	0.27	1.5	ND	53±25	ND
Dec-11	6.1	0.28	1.5	ND	57±50	ND

Notes: S_T = Total settlement (Table 6); S_{V1D} = Average vertical settlement due to volumetric compression using Boulanger and Idriss (2014) (BI-2014), Zhang et al. (2002) (ZRB-2002) procedures and de Greef and Lengkeek (2018) thin-layer correction; $S_{E,L}$ = Ejecta-induced settlement as the difference between the LiDAR-based S_T and S_{V1D}.

Table 8b: Ejecta-Induced settlement for the top 20 m of the soil profile for Patch B for the 50th %ile PGA, P_L=50%, and C_{FC}=0.13 using BI-2014, ZRB-2002, and I_c cutoff of 2.6.

Earthquake Event(s)	M_W	PGA (g)	Depth to Groundwater (m)	S_T (mm)	S_{V1D} (mm)	$S_{E,L}$ (mm)
Sep-10	7.1	0.20	1.5	10±50	62±20	-52±54
Feb-11	6.2	0.45	1.5	163±25	156±50	7±56
Jun-11	6.2	0.27	1.5	22±25	94±25	-72±35
Dec-11	6.1	0.28	1.5	-51±25	98±50	-149±56

Notes: S_T = Total settlement (Table 6); S_{V1D} = Average vertical settlement due to volumetric compression using Boulanger and Idriss (2014) (BI-2014), Zhang et al. (2002) (ZRB-2002) procedures and de Greef and Lengkeek (2018) thin-layer correction; $S_{E,L}$ = Ejecta-induced settlement as the difference between the LiDAR-based S_T and S_{V1D}.

Table 8c: Ejecta-Induced settlement for the top 20 m of the soil profile for Swimming Pool for the 50th %ile PGA, P_L=50%, and C_{FC}=0.13 using BI-2014, ZRB-2002, and I_c cutoff of 2.6.

Earthquake Event(s)	M_W	PGA (g)	Depth to Groundwater (m)	S_T (mm)	S_{V1D} (mm)	$S_{E,L}$ (mm)
Sep-10	7.1	0.20	1.5	ND	44±20	ND
Feb-11	6.2	0.45	1.5	ND	143±50	ND
Jun-11	6.2	0.27	1.5	ND	74±25	ND
Dec-11	6.1	0.28	1.5	ND	78±50	ND

Notes: S_T = Total settlement (Table 6); S_{V1D} = Average vertical settlement due to volumetric compression using Boulanger and Idriss (2014) (BI-2014), Zhang et al. (2002) (ZRB-2002) procedures and de Greef and Lengkeek (2018) thin-layer correction; $S_{E,L}$ = Ejecta-induced settlement as the difference between the LiDAR-based S_T and S_{V1D}.

Table 8d: Ejecta-Induced settlement for the top 20 m of the soil profile for Road within the 20-m buffer for the 50th %ile PGA, P_L=50%, and C_{FC}=0.13 using BI-2014, ZRB-2002, and I_c cutoff of 2.6.

Earthquake Event(s)	M_W	PGA (g)	Depth to Groundwater (m)	S_T (mm)	S_{V1D} (mm)	$S_{E,L}$ (mm)
Sep-10	7.1	0.20	1.5	-4±75	30±20	-34±78
Feb-11	6.2	0.45	1.5	157±25	145±50	12±56
Jun-11	6.2	0.27	1.5	23±25	54±25	-31±35
Dec-11	6.1	0.28	1.5	-20±50	57±50	-77±71

Notes: S_T = Total settlement (Table 6); S_{V1D} = Average vertical settlement due to volumetric compression using Boulanger and Idriss (2014) (BI-2014), Zhang et al. (2002) (ZRB-2002) procedures and de Greef and Lengkeek (2018) thin-layer correction; $S_{E,L}$ = Ejecta-induced settlement as the difference between the LiDAR-based S_T and S_{V1D}.

Note 3: The uncertainty for volumetric settlement was derived based on the sensitivity of volumetric settlement to PGA, C_{FC}, and P_L for each earthquake event for VsVp 57203 *Shirley Intermediate School* and CC LIQ 1 – CPT 5586 – *Vivian St* sites. Taking the 50th percentile as the baseline case, the minimum and maximum values corresponding to the difference between the 25th percentile and the 50th percentile and the 75th percentile and the 50th percentile were determined. The arithmetic mean of the range of the minimum and maximum difference was evaluated for each patch at the two sites. The maximum arithmetic mean for each earthquake event was rounded to the nearest five and used as the uncertainty value. Accordingly, the 1-D volumetric settlement uncertainties of ±20, ±50, ±25, and ±50 mm for the Sep-10, Feb-11, Jun-11, and Dec-11 earthquake events, respectively, were used for all sites in this study.

Table 9a: Coverage area and height of ejecta estimates for Patch A using photographs.

Earthquake Event	$A_{E,thick}$ (m^2)	$H_{E,thick}$ (mm)	$A_{E,thin}$ (m^2)	$H_{E,thin}$ (mm)	A_T (m^2)
Sep-10	0	0	0	0	25.3
Feb-11	0	0	0	0	25.3
Jun-11	0	0	0	0	25.3
Dec-11	0	0	0	0	25.3

Notes: $A_{E,thick/thin}$ = Coverage area of thick/thin ejecta layers; $H_{E,thick/thin}$ = Lower-upper estimate of height of thick/thin ejecta layers; A_T = Total assessment area of a buffer being considered; Thin and thick layers correspond to light gray and dark gray colors of ejecta observed in aerial photographs.

Table 9b: Coverage area and height of ejecta estimates for Patch B using photographs.

EQ Event	$H_{E,thick1}$ (mm)	$A_{E,thick1}$ (m^2)	$H_{E,thick2}$ (mm)	$A_{E,thick2}$ (m^2)	$H_{E,thin1}$ (mm)	$A_{E,thin1}$ (m^2)	$H_{E,thin2}$ (mm)	$A_{E,thin2}$ (m^2)	A_T (m^2)
Sep-10	0	0	40-70	2.2	20-50	40.2	0	0	42.4
Feb-11	100-140	6.8	80-120	5.2	60-100	8.3	5-10	21.8	42.1
Jun-11	0	0	0	0	50-100	8.1	5-10	7.1	22.9*
Dec-11	0	0	0	0	0	0	0	0	42.4

Notes: $A_{E,thick/thin}$ = Coverage area of thick/thin ejecta layers; $H_{E,thick/thin}$ = Lower-upper estimate of height of thick/thin ejecta layers; Thin and thick layers correspond to light gray and dark gray colors of ejecta observed in aerial photographs; A_T = Total assessment area of a buffer being considered; * indicates reduction in A_T due to the presence of shadows.

Table 9c: Coverage area and height of ejecta estimates for Swimming Pool using photographs.

Earthquake Event	$A_{E,thick}$ (m^2)	$H_{E,thick}$ (m)	$A_{E,thin}$ (m^2)	$H_{E,thin}$ (m)	A_T (m^2)
Sep-10	0	0	0	0	44.6
Feb-11	44.6	500-1000	0	0	44.6
Jun-11	NA	NA	NA	NA	44.6
Dec-11	0	0	0	0	44.6

Notes: $A_{E,thick/thin}$ =Coverage area of thick/thin ejecta layers; $H_{E,thick/thin}$ = Lower-upper estimate of height of thick/thin ejecta layers; A_T= Total assessment area of a buffer being considered; Thin and thick layers correspond to light gray and dark gray colors of ejecta observed in aerial photographs; ND = Not determined due to the evident presence of ejecta from the Feb-11 EQ and the presence of shadows in the aerial photograph for the Jun-11 EQ across almost the entire assessment area.

Table 9d: Coverage area and height of ejecta estimates for Road (50-m buffer) using photographs.

EQ Event	$H_{E,prism/pyr}$ (mm)	$V_{E,prism+pyr}$ (m^3)	$H_{E,thin}$ (mm)	$A_{E,thin}$ (m^2)	$H_{E,thick}$ (mm)	$A_{E,thick}$ (m^2)	A_T (m^2)
Sep-10	13-180	11.0-16.0	2-6	274	20-40	2.7	565
Feb-11	13-180	22.1-35.0	3-6	129	0	0	562
Jun-11	20-180	14.7-23.8	3-6	154	0	0	478*
Dec-11	8-180	4.25-5.23	5-10	80.3	10-30	9.2	563*

Notes: $H_{E,prism/pyr}$ = Lower-upper estimate of ejecta height near the curb based on 2-4% cross slope of normal crown; $V_{E,prism+pyr}$ = Lower-upper estimate of total volume of prismatic- and pyramidal-shape ejecta; $A_{E,thin/thick}$ =Coverage area of thin/thick ejecta layers; $H_{E,thin/thick}$ = Lower-upper estimate of height of thin/thick ejecta layers; A_T= Total assessment area of a buffer being considered; * indicates reduction in A_T due to the presence of shadows/objects.

Note 4: The values in Table 9 correspond to the coverage area of ejecta outlined in aerial photographs (Figures 68-71) and the lower and upper estimates of ejecta height based on geometrical approximations, ground photographs (Figures 74, 77, 78, 81, and 82), and EQC LDAT property inspection reports (e.g., Figures 72, 73, 75, 76, 79, and 80). The ejecta-induced settlement using photographs and engineering judgment, $S_{E,P}$, is estimated as

$$S_{E,P} = \frac{\sum_{i=1}^{a} A_{E,thick,i} * H_{E,thick,i} + \sum_{j=1}^{b} A_{E,thin,j} * H_{E,thin,j}}{A_T} + \frac{\frac{1}{2}\sum_{n=1}^{f} W_{E,prism,n} * H_{E,prism,n} * L_{E,prism,n}}{A_T} + \frac{\frac{1}{3}\sum_{p=1}^{g} W_{E,r.pyramid,p} * H_{E,r.pyramid,p} * L_{E,r.pyramid,p}}{A_T} + \frac{\frac{1}{6}\sum_{r=1}^{h} W_{E,t.pyramid,r} * H_{E,t.pyramid,r} * L_{E,t.pyramid,r}}{A_T} = \frac{\sum_{i=1}^{a} V_{E,thick,i} + \sum_{j=1}^{b} V_{E,thin,j} + \sum_{n=1}^{f} V_{E,prism,n} + \sum_{p=1}^{g} V_{E,r.pyramid,p} + + \sum_{r=1}^{h} V_{E,t.pyramid,r}}{A_T}$$

where

- $A_{E,thick,i}$ and $H_{E,thick,i}$ are the area and the height of a thick ejecta layer, respectively;
- $A_{E,thin,j}$ and $H_{E,thin,j}$ are the area and the height of a thin ejecta layer, respectively;
- $W_{E,prism,n}$ and $L_{E,prism,n}$ are the width and the length, respectively, of the coverage area of a prismatically shaped ejecta layer, respectively, and $H_{E,prism,n}$ is the height of a prism-like ejecta layer;
- $W_{E,r.pyr,p}$ and $L_{E,r.pyr,p}$ are the width and the length, respectively, of the coverage area of an ejecta layer shaped as a rectangular-base pyramid, and $H_{E,r.pyr,p}$ is the height of the rectangular-base pyramid-like ejecta layer;
- $W_{E,t.pyr,r}$ and $L_{E,t.pyr,r}$ are the width and the length, respectively, of the coverage area of an ejecta layer shaped as a triangular-base pyramid, and $H_{E,t.pyr,r}$ is the height of the triangular-base pyramid-like ejecta layer;
- A_T is the total assessment area for a buffer being considered (Figure 1).

Table 10a: Ejecta-induced settlement estimates for Patches A and B based on photographs.

Earthquake Event	Patch A (10-, 20-, and 50-m buffers)		Patch B (50-m buffer)	
	$S_{E,P,lower}$ (mm)	$S_{E,P,upper}$ (mm)	$S_{E,P,lower}$ (mm)	$S_{E,P,upper}$ (mm)
Sep-10	0	0	21	51
Feb-11	0	0	40	62
Jun-11	0	0	19	39
Dec-11	0	0	0	0

Note: $S_{E,P,lower}$ and $S_{E,P,upper}$ correspond to lower and upper estimates of $S_{E,P}$, respectively.

Table 10b: Ejecta-induced settlement estimates for Swimming Pool and Road based on photographs.

Earthquake Event	Swimming Pool (50-m buffer)		Road (50-m buffer)	
	$S_{E,P,lower}$ (mm)	$S_{E,P,upper}$ (mm)	$S_{E,P,lower}$ (mm)	$S_{E,P,upper}$ (mm)
Sep-10	0	0	21	31
Feb-11	500	1000	40	64
Jun-11	ND	ND	32	52
Dec-11	0	0	9	11

Note: $S_{E,P,lower}$ and $S_{E,P,upper}$ correspond to lower and upper estimates of $S_{E,P}$, respectively; ND= Not determined due to the evident presence of ejecta from the Feb-11 EQ and the presence of shadows in the aerial photograph for the Jun-11 EQ across almost the entire assessment area.

Table 11a: Best final estimates of ejecta-induced settlement for Patches A and B.

EQ Event	Patch A (10-, 20-, and 50-m buffers)			Patch B (50-m buffer)		
	$S_{E,L}$ (mm)	$S_{E,P}$ (mm)	$S_{E,final}$ (mm)	$S_{E,L}$ (mm)	$S_{E,P}$ (mm)	$S_{E,final}$ (mm)
Sep-10	ND	0	0	-52±54	36±15	35±15
Feb-11	ND	0	0	7±56	52±12	50±10
Jun-11	ND	0	0	-72±35	29±10	30±10
Dec-11	ND	0	0	-149±56	0	0

Notes: $S_{E,L}$ = Ejecta-induced settlement based on LiDAR data reported in Table 8; $S_{E,P}$ = Median ejecta-induced settlement for the range of values reported in Table 10; $S_{E,final}$ = Best final estimate of ejecta-induced settlement rounded to the nearest 5; Final plus/minus values are also rounded to the nearest 5.

Table 11b: Best final estimates of ejecta-induced settlement for Swimming Pool and Road.

Earthquake Event	Swimming Pool (50-m buffer)			Road (50-m buffer)		
	$S_{E,L}$ (mm)	$S_{E,P}$ (mm)	$S_{E,final}$ (mm)	$S_{E,L}$ (mm)	$S_{E,P}$ (mm)	$S_{E,final}$ (mm)
Sep-10	ND	0	0	-34±78	26±5	25±5
Feb-11	ND	750±250	750±250	12±56	52±11	50±10
Jun-11	ND	ND	ND	-31±35	42±10	40±10
Dec-11	ND	0	0	-77±71	10±1	10±5

Notes: $S_{E,L}$ = Ejecta-induced settlement based on LiDAR data reported in Table 8; $S_{E,P}$ = Median ejecta-induced settlement for the range of values reported in Table 10; $S_{E,final}$ = Best final estimate of ejecta-induced settlement rounded to the nearest 5; Final plus/minus values are also rounded to the nearest 5; ND= Not determined.

Note 5:

- Patch A: $S_{E,final}$ is based solely on $S_{E,P}$ for all earthquake events due to the evident absence of ejecta.
- Patch B: $S_{E,final}$ is based solely on $S_{E,P}$ for all earthquake events due to the negative $S_{E,L}$ values for the Sep-10, Jun-11, and Dec-11 EQs and the evident absence of ejecta for the Dec-11 EQ. For the Feb-11 EQ, $S_{E,L}$ is negligible compared to $S_{E,P}$, which is based on the physical evidence.
- Swimming Pool: $S_{E,final}$ is based solely on $S_{E,P}$ for all earthquake events.
- Road: $S_{E,final}$ is based solely on $S_{E,P}$ for all earthquake events due to the negative $S_{E,L}$ values for the Sep-10, Jun-11, and Dec-11 EQs. For the Feb-11 EQ, $S_{E,L}$ is negligible compared to $S_{E,P}$, which is based on the physical evidence.
- The 31 Landy St site is not in the apparent zone of higher/lower ground surface subsidence for the Sep-10 or Feb-11 EQ. The site is in the zone of accurate LPI prediction of liquefaction severity for the Sep-10 and Feb-11 EQ (Maurer et al. 2014[3]). The LDAT inspection reports and ground photographs are available for the properties with Patches A and B and Swimming Pool. The inspection team did not observe ejecta within Patch A. The team did observe ejecta within Patch B at the time of the inspection (13 Oct 2010 and 17 June 2011). The maximum ejecta height at the time of the 17 June 2011 inspection was recorded as ~200 mm (at ~5% of the property). No ejecta height measurements were taken at the time of the 13 Oct 2010 inspection. The ejecta height at other properties within the 50-m buffer ranged from 100 mm to 300 mm. Ejecta were mostly located around the buildings as compared to the open field (i.e., front and back yards). The height of ejecta in the swimming pool ranged from ~500 mm to ~1000 mm. There are no ground photographs of ejecta on the road.

Summary 1:

- **The best estimate of the ejecta-induced free-field ground settlement at the 31 Landy St site for the SEP 2010, FEB 2011, JUN 2011, and DEC 2011 earthquake is 35±15 mm, 50±10 mm, 30±10 mm, and 0 mm, respectively.**

[3] Maurer, B. W., Green, R. A., Cubrinovski, M., & Bradley, B. A. (2014). Evaluation of the Liquefaction Potential Index for Assessing Liquefaction Hazard in Christchurch, New Zealand. *Journal of Geotechnical and Geoenvironmental Engineering*, 140(7), 04014032-1-11. doi:10.1061/(asce)gt.1943-5606.0001117

- **The best estimate of the ejecta-induced settlement of the road at the 31 Landy St site for the SEP 2010, FEB 2011, JUN 2011, and DEC 2011 earthquake is 25±5 mm, 50±10 mm, 40±10 mm, and 10±5 mm, respectively.**

Figure 4: Location of the site.

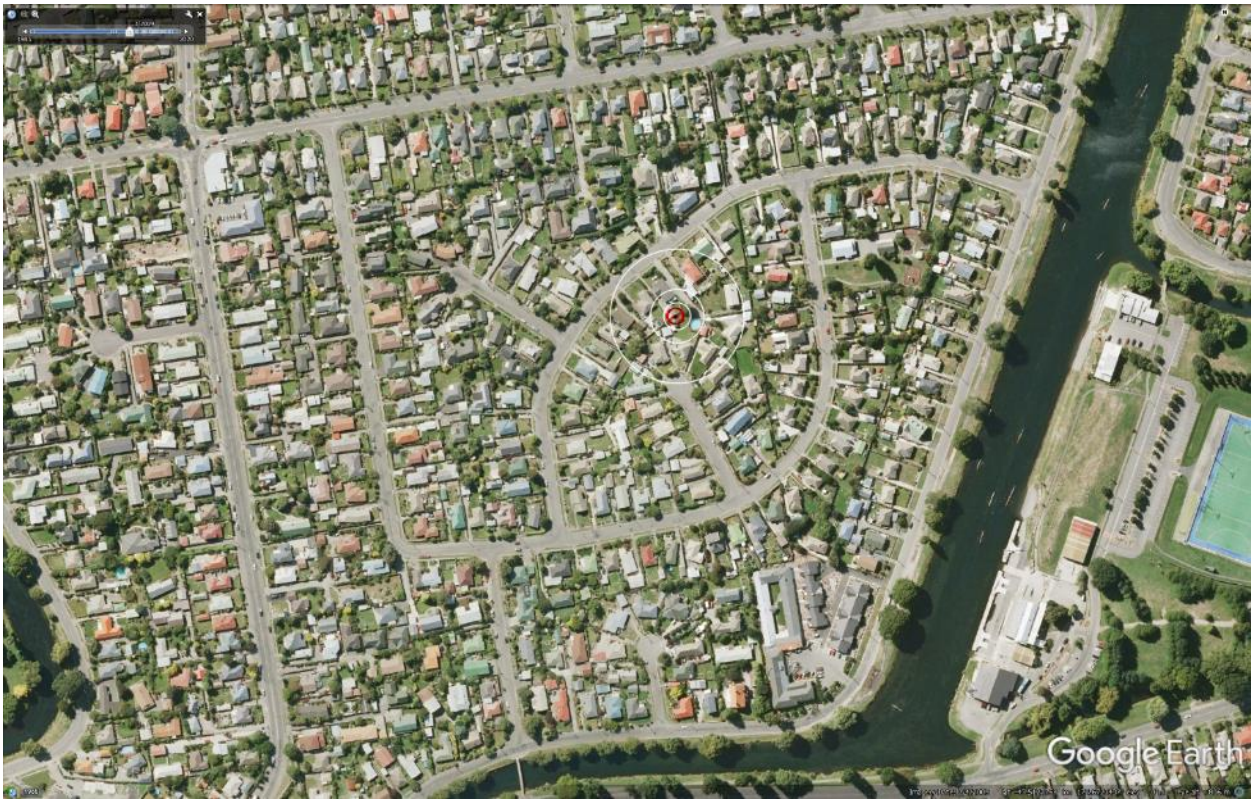

Figure 5: Position of the site relative to nearby buildings, vegetation, and free-face features.

Figure 6: Street view of the flat land.

Figure 7: Satellite image of the site taken in Dec 2004.

Figure 8: Satellite image of the site taken in Mar 2009.

Figure 9: Satellite image of the site taken on Sep 3, 2010.

Figure 10: Satellite image of the site taken on Sep 5, 2010.

Figure 11: Satellite image of the site taken on Feb 7, 2011.

Figure 12: Satellite image of the site taken on Feb 23, 2011.

Figure 13: Satellite image of the site taken on Feb 26, 2011.

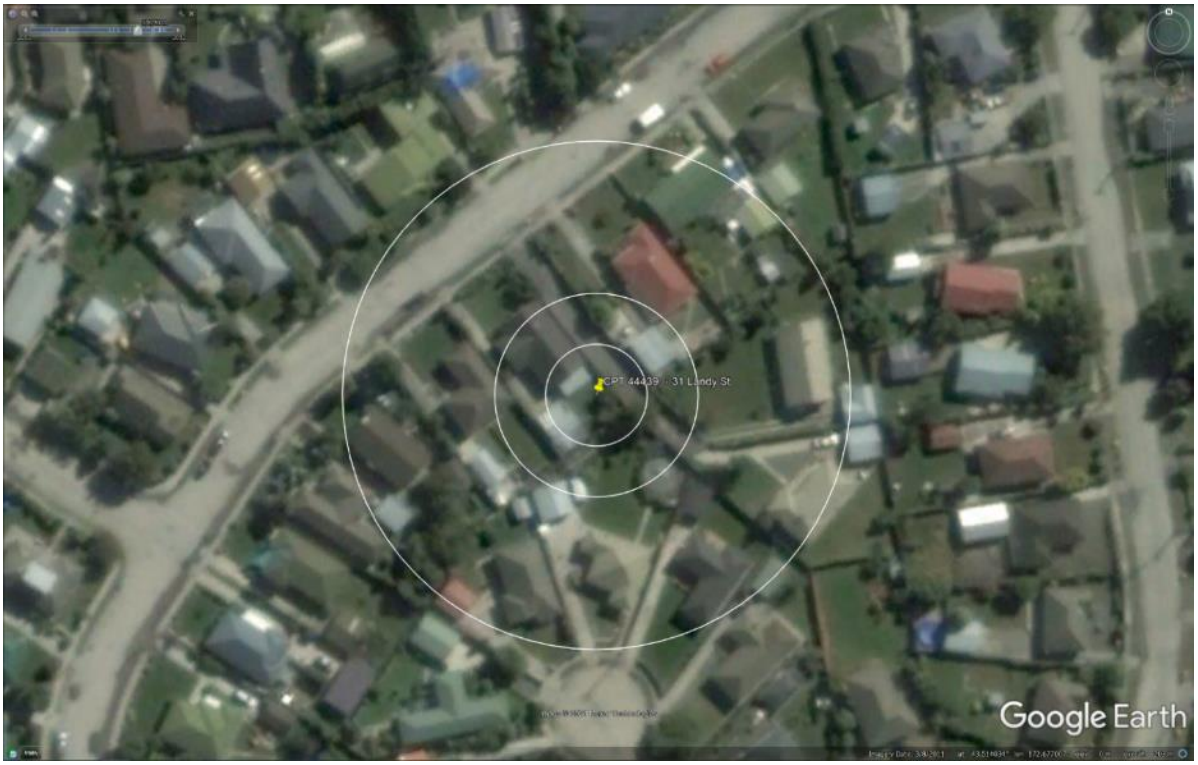

Figure 14: Satellite image of the site taken on Mar 8, 2011. It appears that some ejecta from the Feb-11 EQ remained at the site.

Figure 15: Satellite image of the site taken in Apr 2012.

Figure 16: Satellite image of the site taken in Oct 2012.

Figure 17: Satellite image of the site taken in Mar 2013.

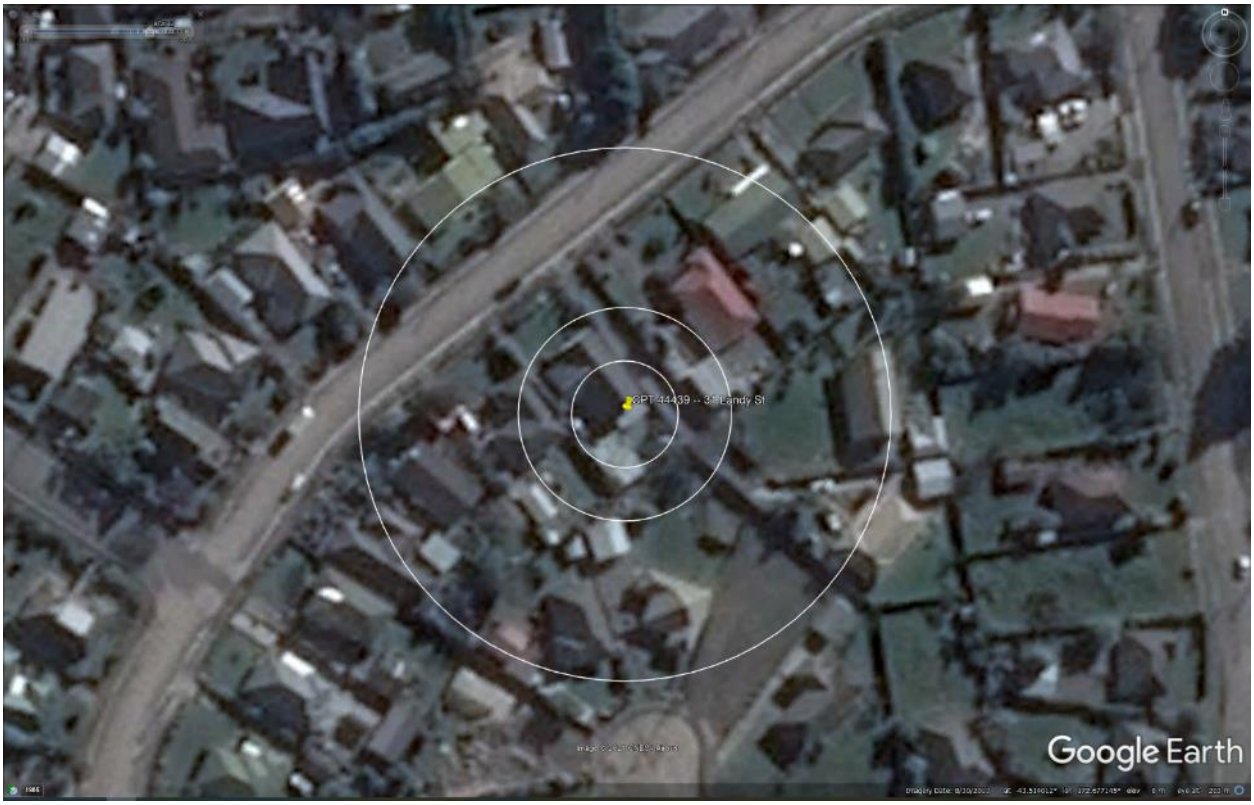

Figure 18: Satellite image of the site taken in Aug 2013.

Figure 19: Satellite image of the site taken in Feb 2014.

Figure 20: Satellite image of the site taken in Mar 2014.

Figure 21: Satellite image of the site taken in Aug 2014.

Figure 22: Satellite image of the site taken in Sep 2014.

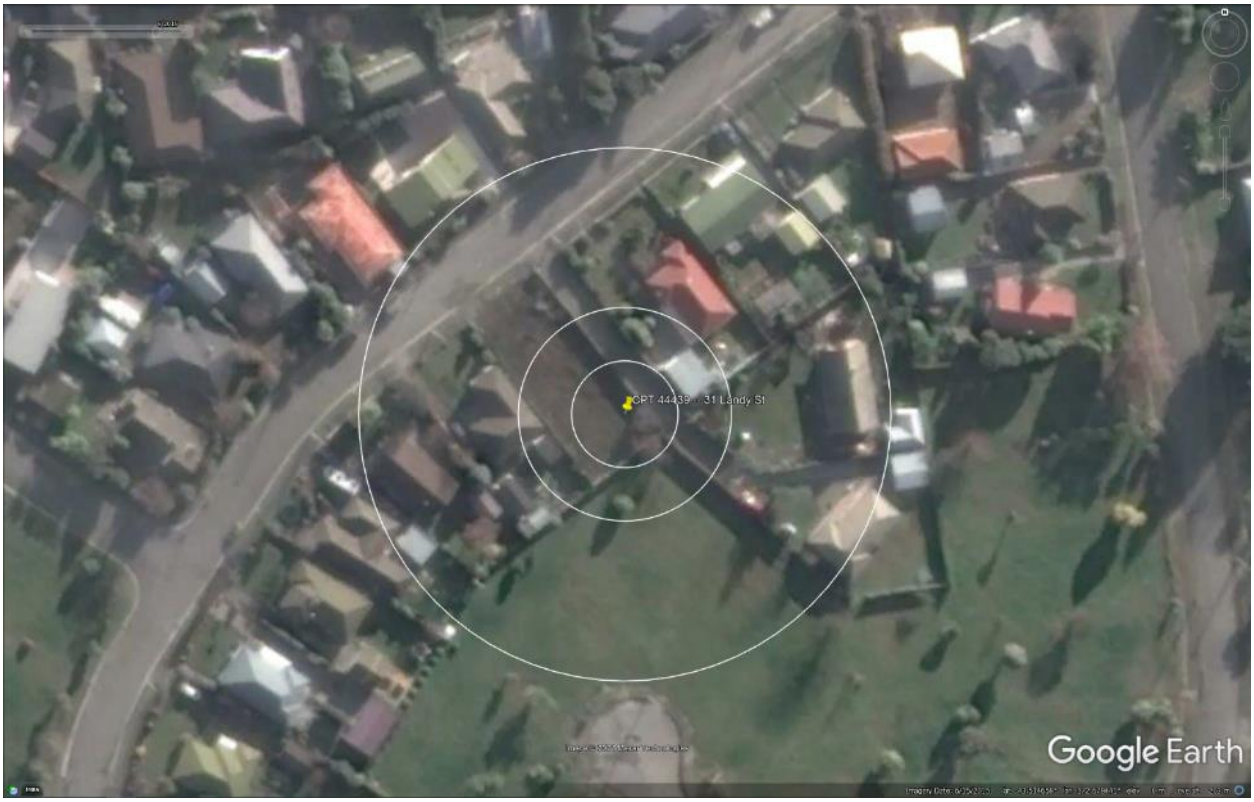

Figure 23: Satellite image of the site taken in Jun 2015.

Figure 24: Satellite image of the site taken in July 2015.

Figure 25: Satellite image of the site taken in Sep 2015.

Figure 26: Satellite image of the site taken in Nov 2015.

Figure 27: Aerial photograph of the site taken on Sep 4, 2010.

Figure 28: Aerial photograph of the site taken on Feb 24, 2011.

Figure 29: Aerial photograph of the site taken on June 14-15, 2011.

Figure 30: Aerial photograph of the site taken on June 16, 2011.

Figure 31: Aerial photograph of the site taken on Dec 24, 2011.

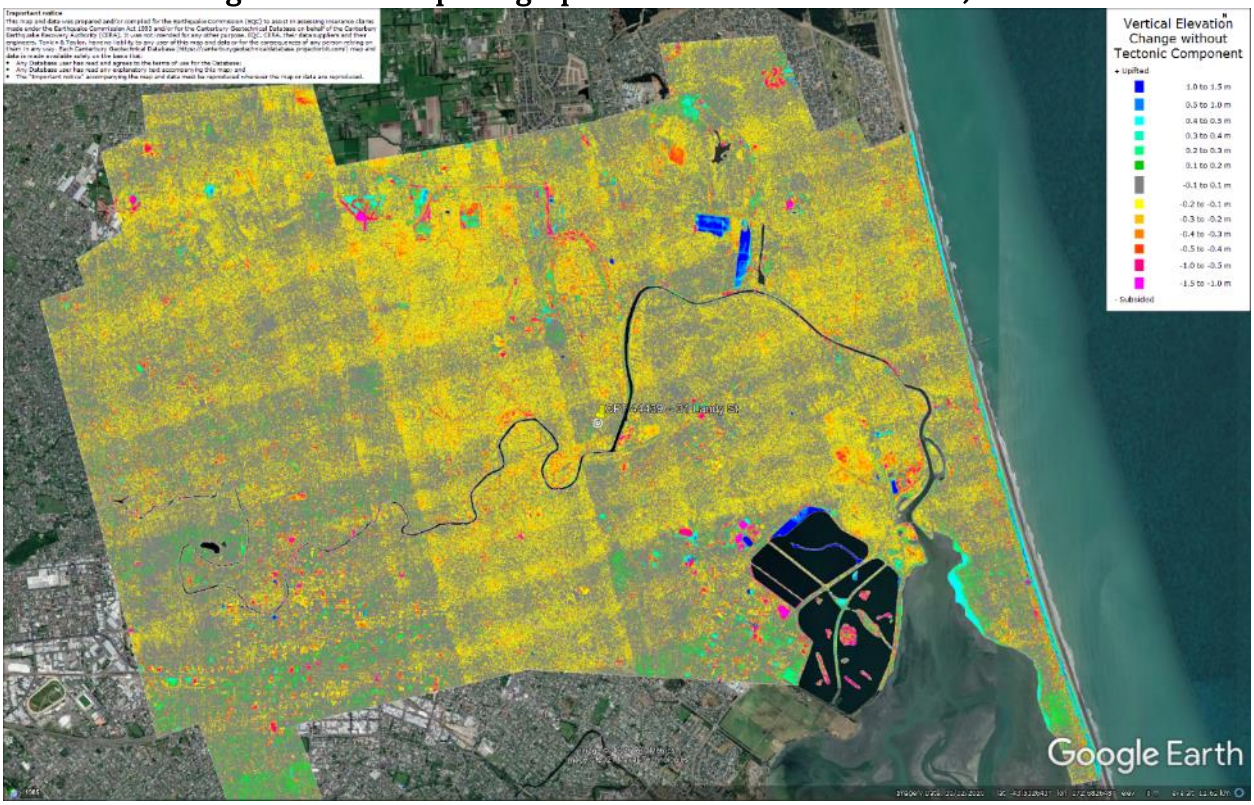

Figure 32: Vertical Ground Movements (Surface – Tectonic) for Sep 2010 Earthquake – the site is not in the apparent zone of overestimated ground surface subsidence.

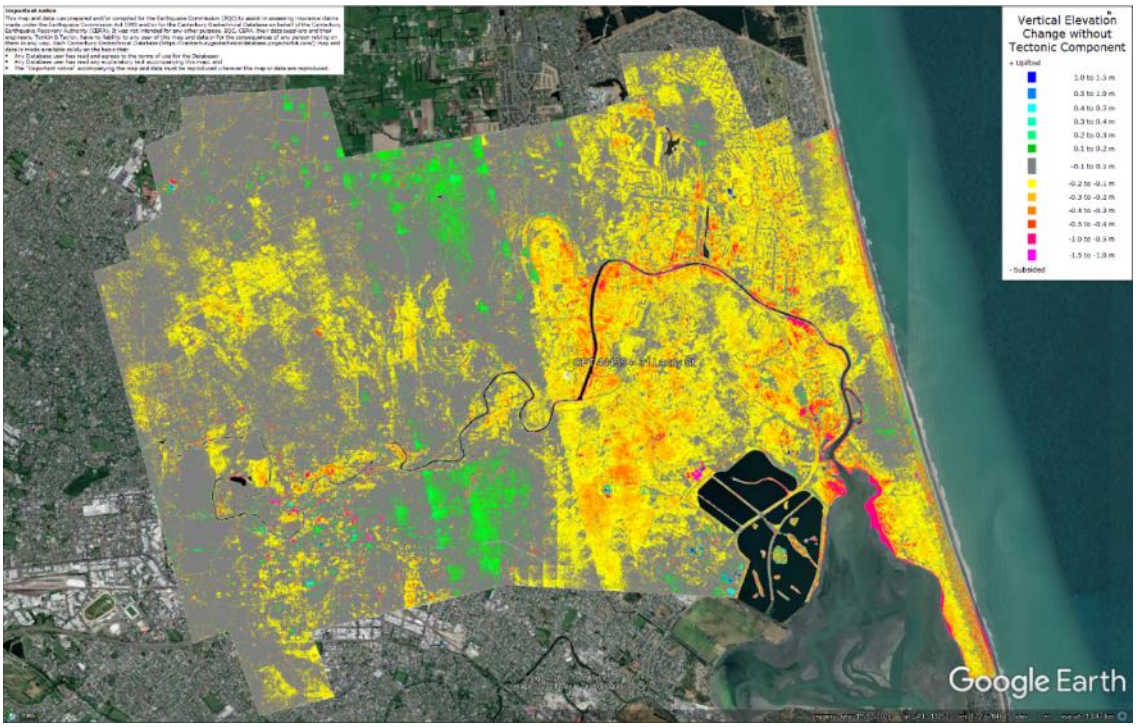

Figure 33: Vertical Ground Movements (Surface – Tectonic) for Feb 2011 Earthquake – the site is not in the apparent zone of underestimated ground surface subsidence.

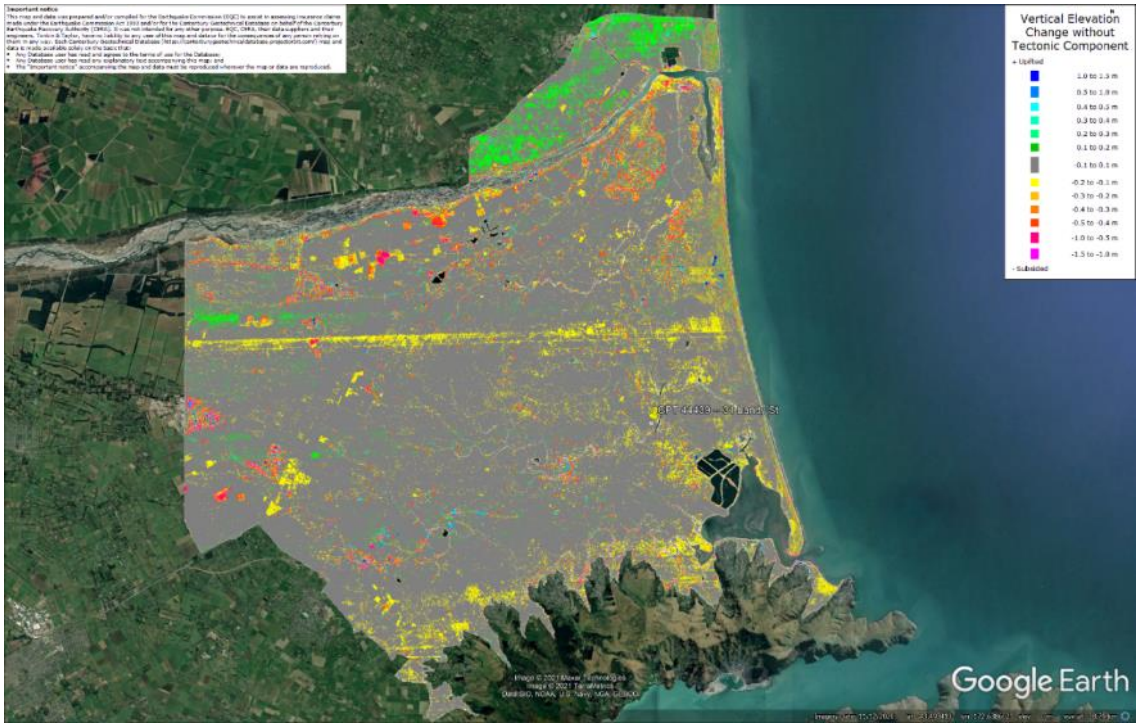

Figure 34: Vertical Ground Movements (Surface – Tectonic) for June 2011 Earthquake – the site is not in the apparent zone of overestimated/underestimated ground surface subsidence.

Figure 35: Vertical Ground Movements (Surface – Tectonic) for Dec 2011 Earthquake – the site is not in the apparent zone of overestimated/underestimated ground surface subsidence.

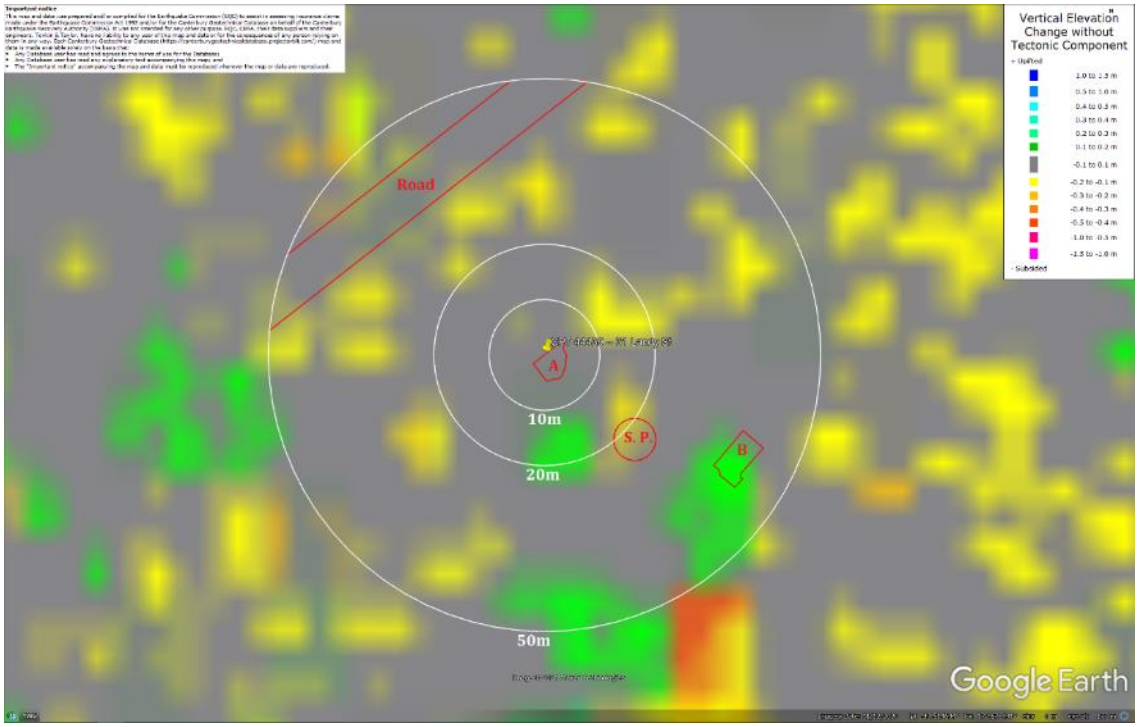

Figure 36: Ground surface subsidence without tectonic component for Sep 2010 Earthquake according to the LiDAR DEM.

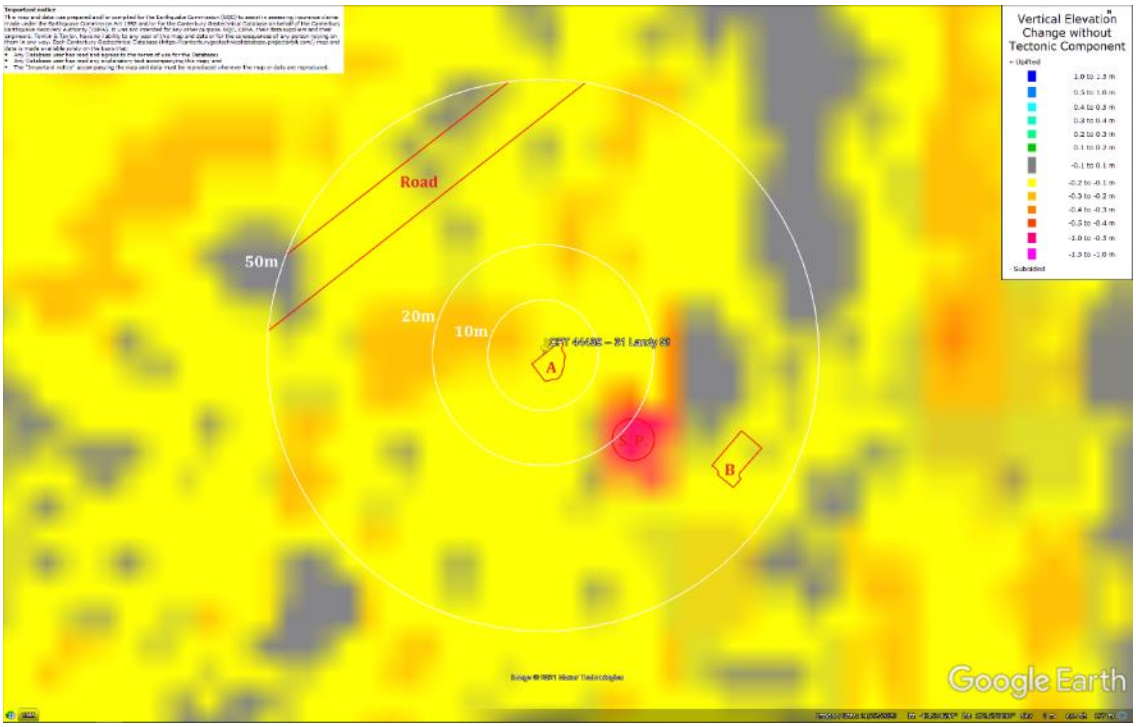

Figure 37: Ground surface subsidence without tectonic component for Feb 2011 Earthquake according to the LiDAR DEM.

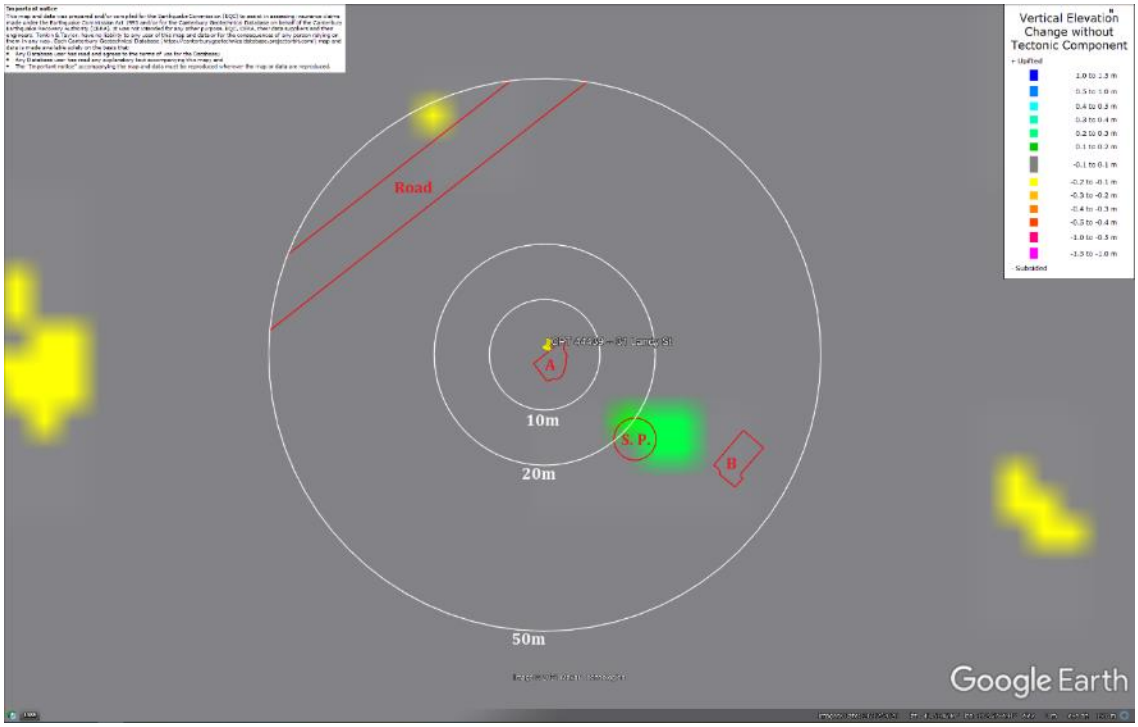

Figure 38: Ground surface subsidence without tectonic component for June 2011 Earthquake according to the LiDAR DEM.

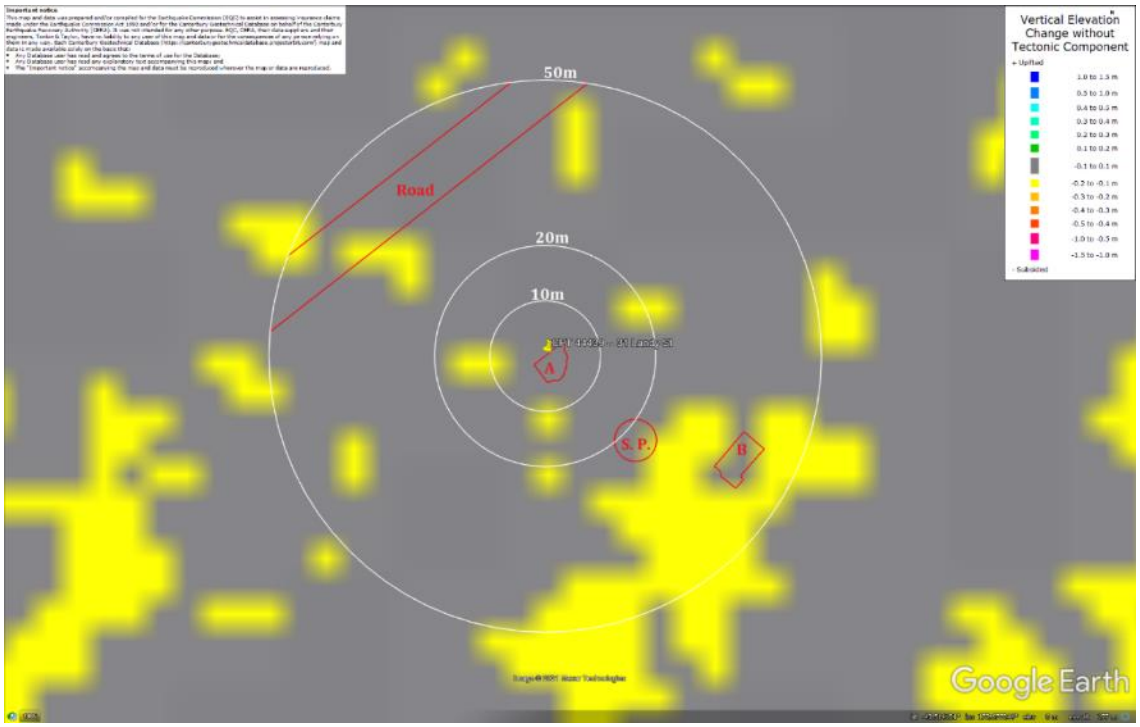

Figure 39: Ground surface subsidence without tectonic component for Dec 2011 Earthquake according to the LiDAR DEM.

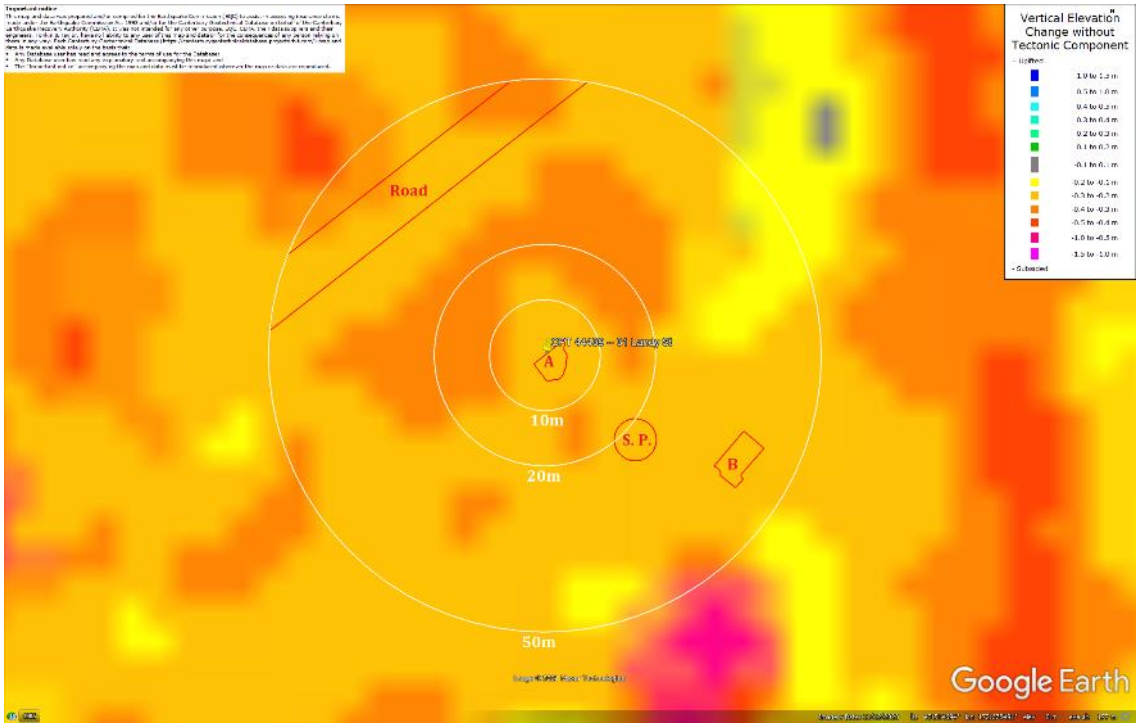

Figure 40: Ground surface subsidence without tectonic component for Canterbury Earthquake Sequence according to the LiDAR DEM.

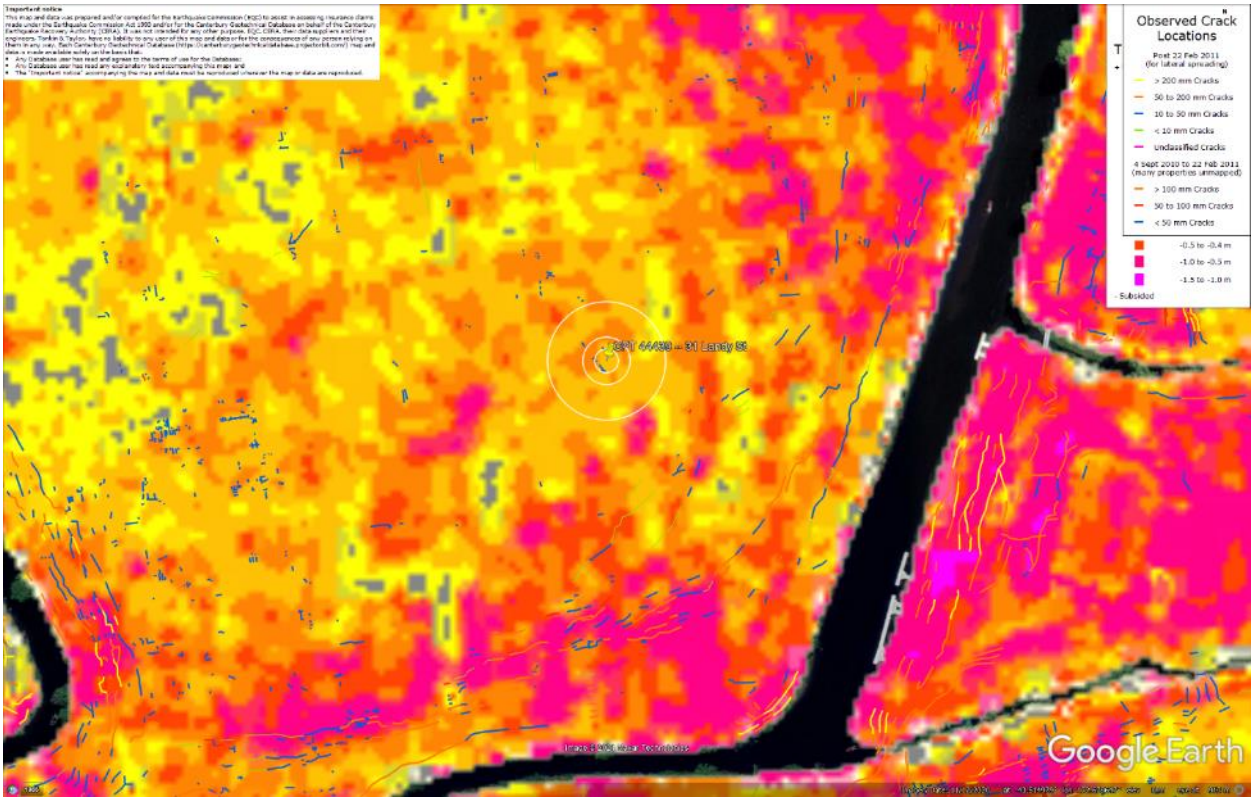

Figure 41: No lateral spreading for Canterbury Earthquake Sequence.

Figure 42: Vertical tectonic movements for Sep 2010 Earthquake.

Figure 43: Vertical tectonic movements for Feb 2011 Earthquake.

Figure 44: Vertical tectonic movements for June 2011 Earthquake.

Figure 45: Vertical tectonic movements for Dec 2011 Earthquake.

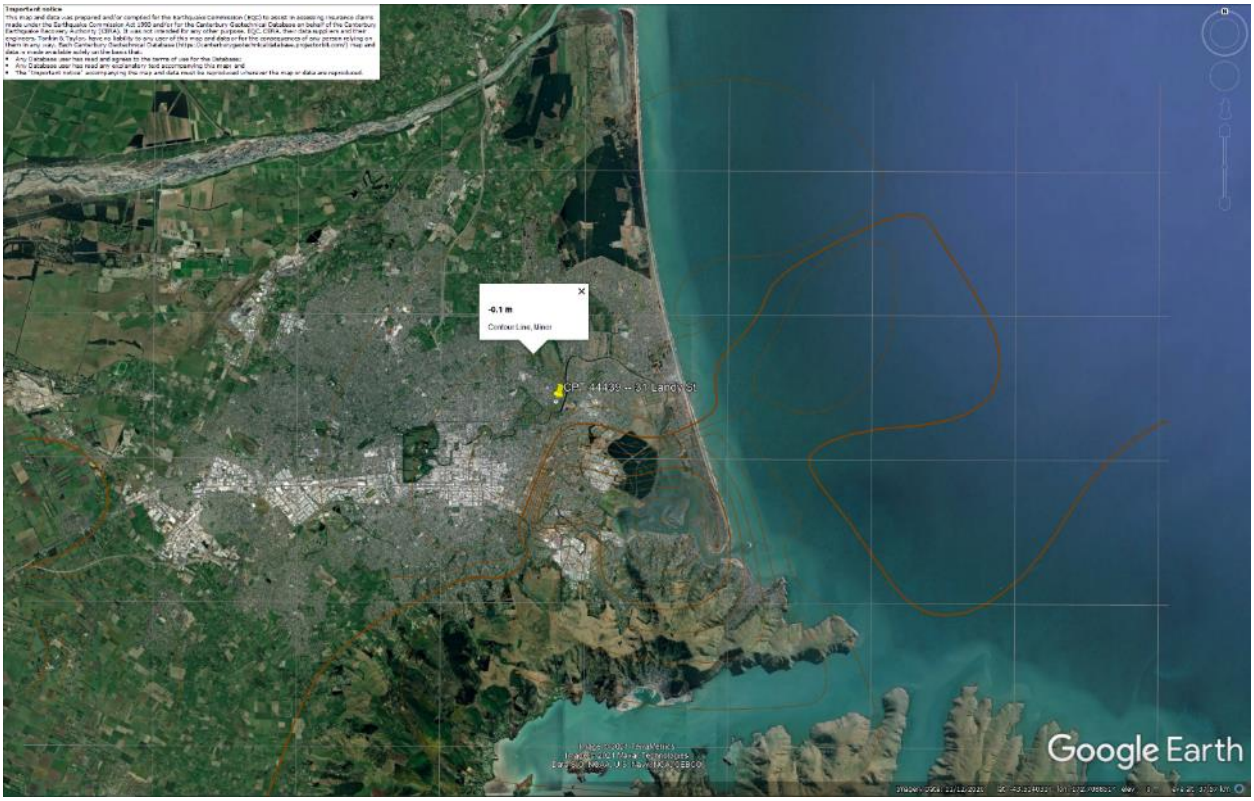

Figure 46: Vertical tectonic movements for Canterbury Earthquake Sequence.

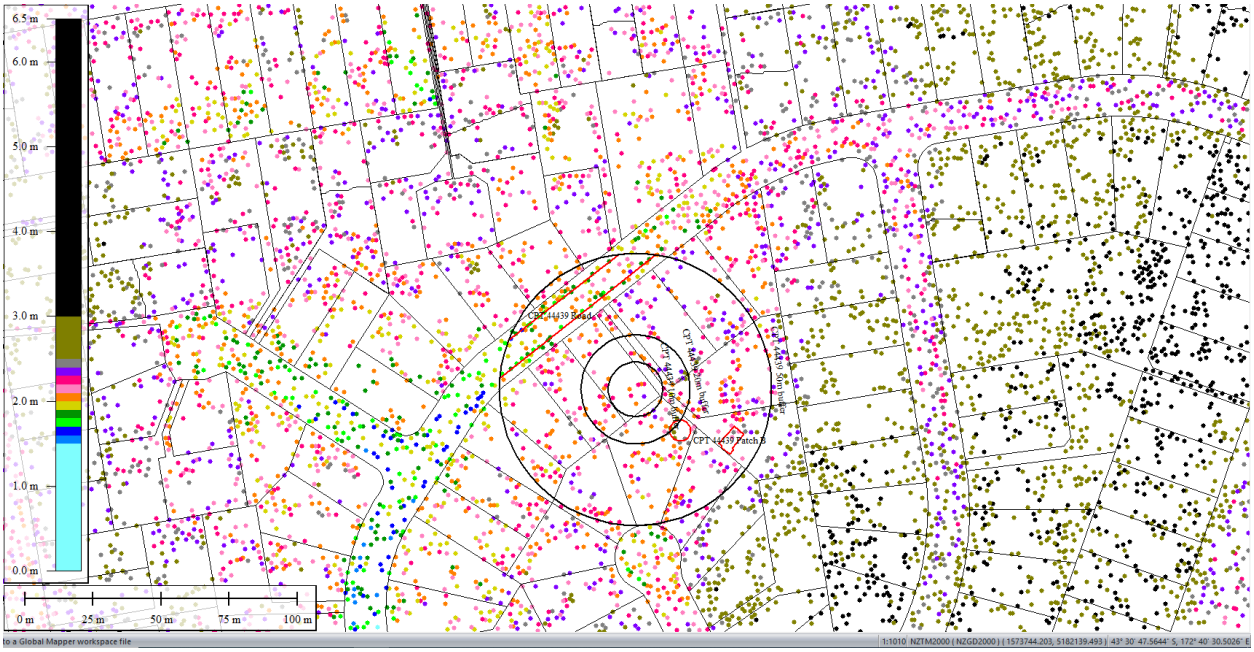

Figure 47: Jul 2003 LiDAR survey.

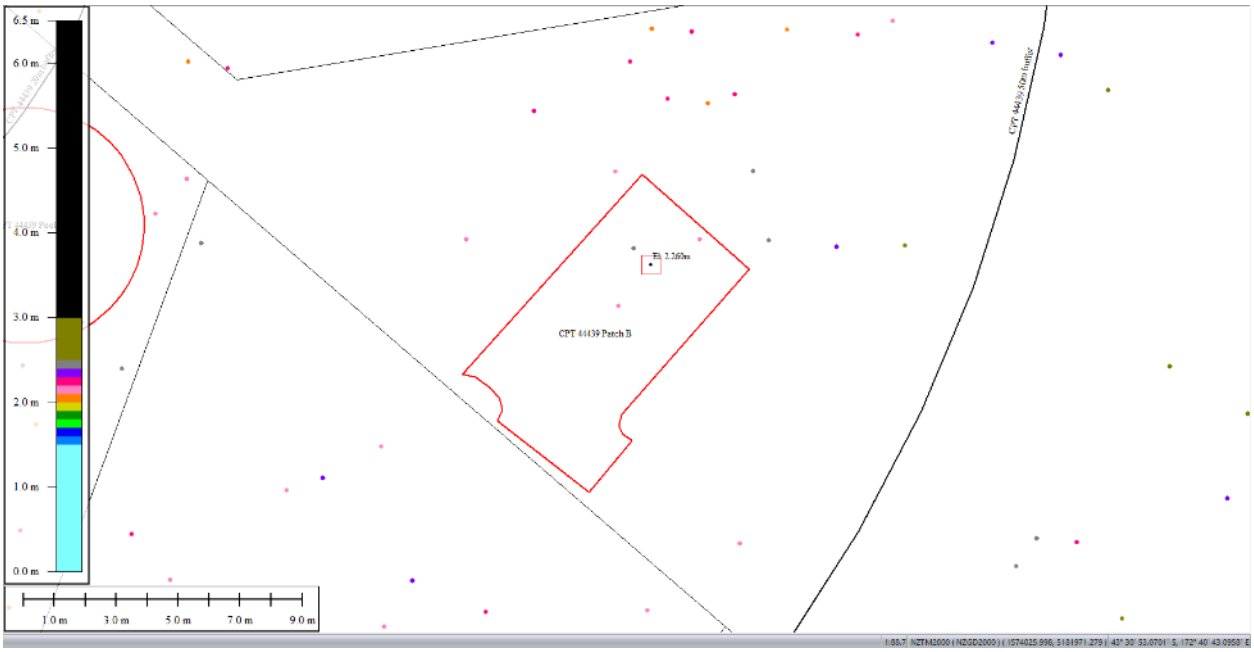

Figure 48: Ground surface elevation averaged over 50-m buffer for Patch B for Jul 2003 LiDAR survey.

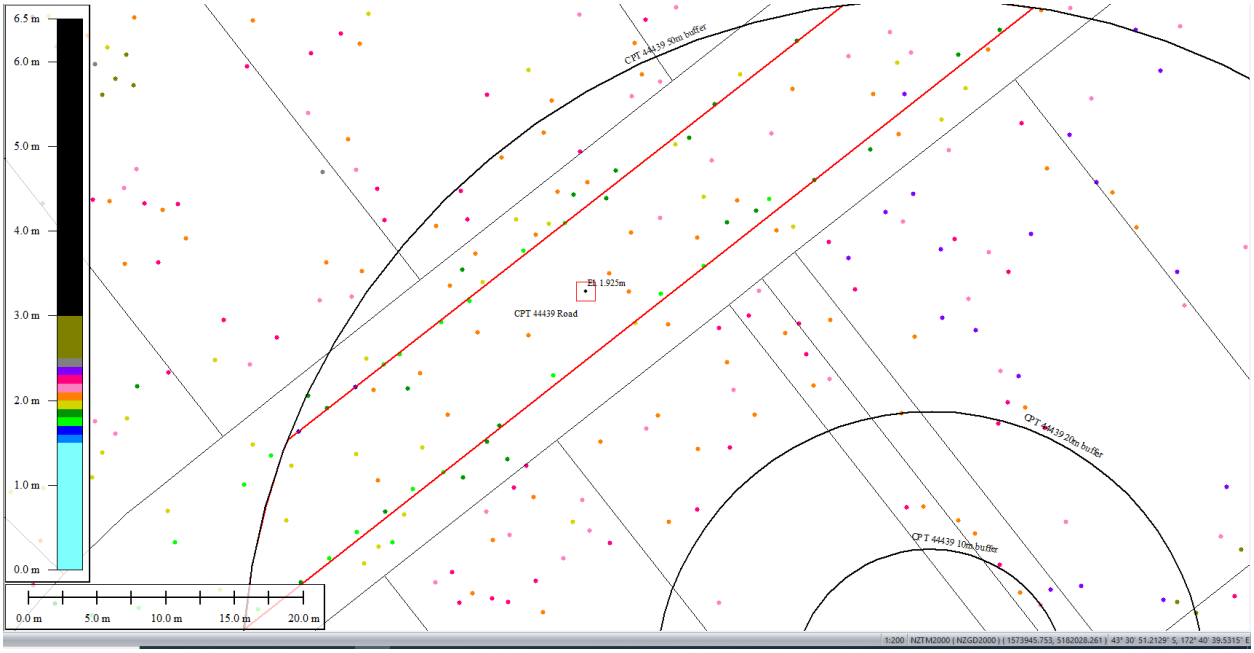

Figure 49: Ground surface elevation averaged over 50-m buffer for Road for Jul 2003 LiDAR survey.

Figure 50: Sep 5, 2010 LiDAR survey.

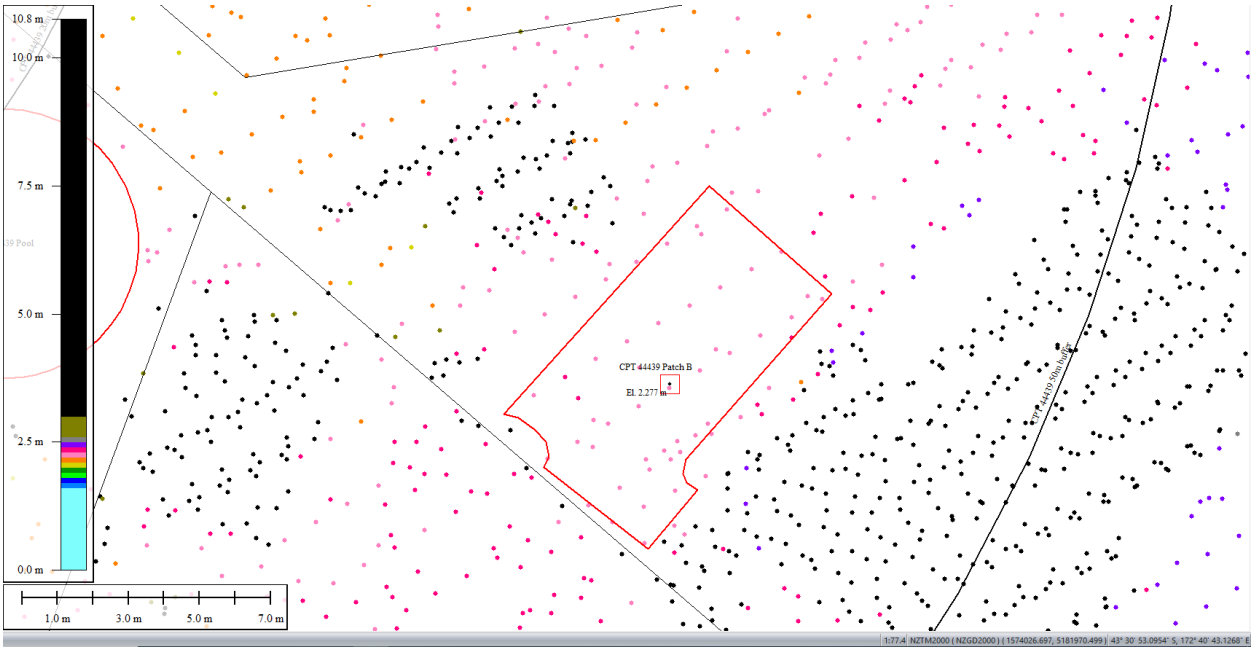

Figure 51: Ground surface elevation averaged over 50-m buffer for Patch B for Sep 5, 2010, LiDAR survey.

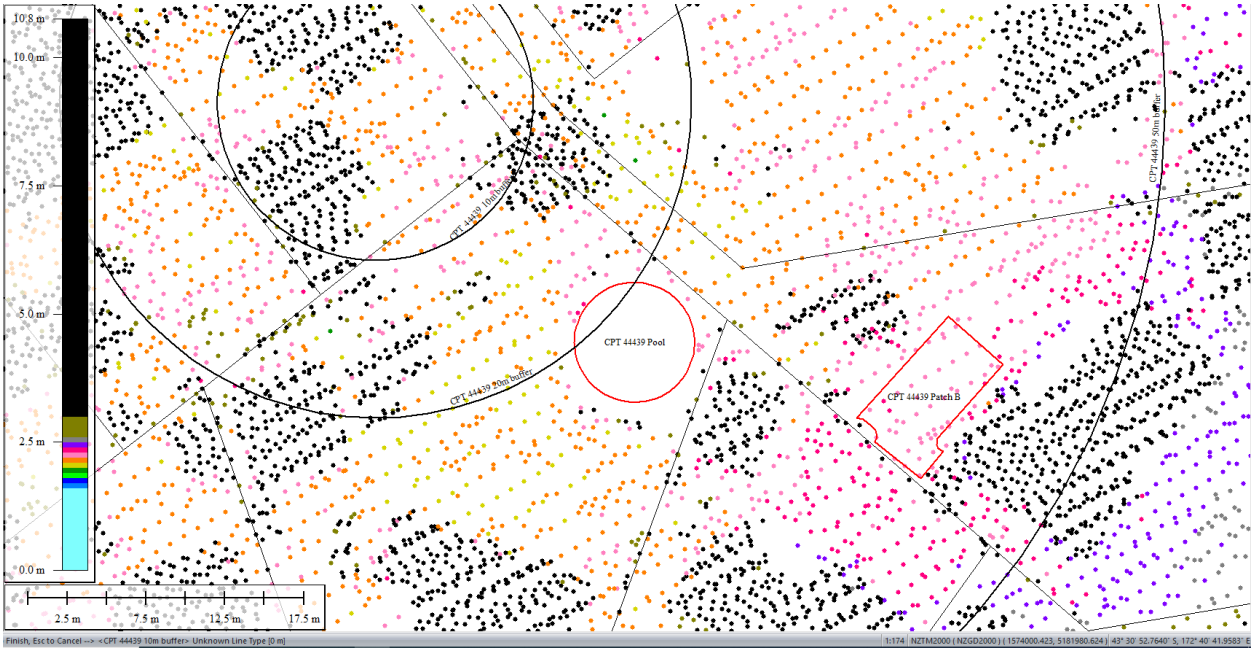

Figure 52: Ground surface elevation averaged over 50-m buffer for Swimming Pool for Sep 5, 2010, LiDAR survey.

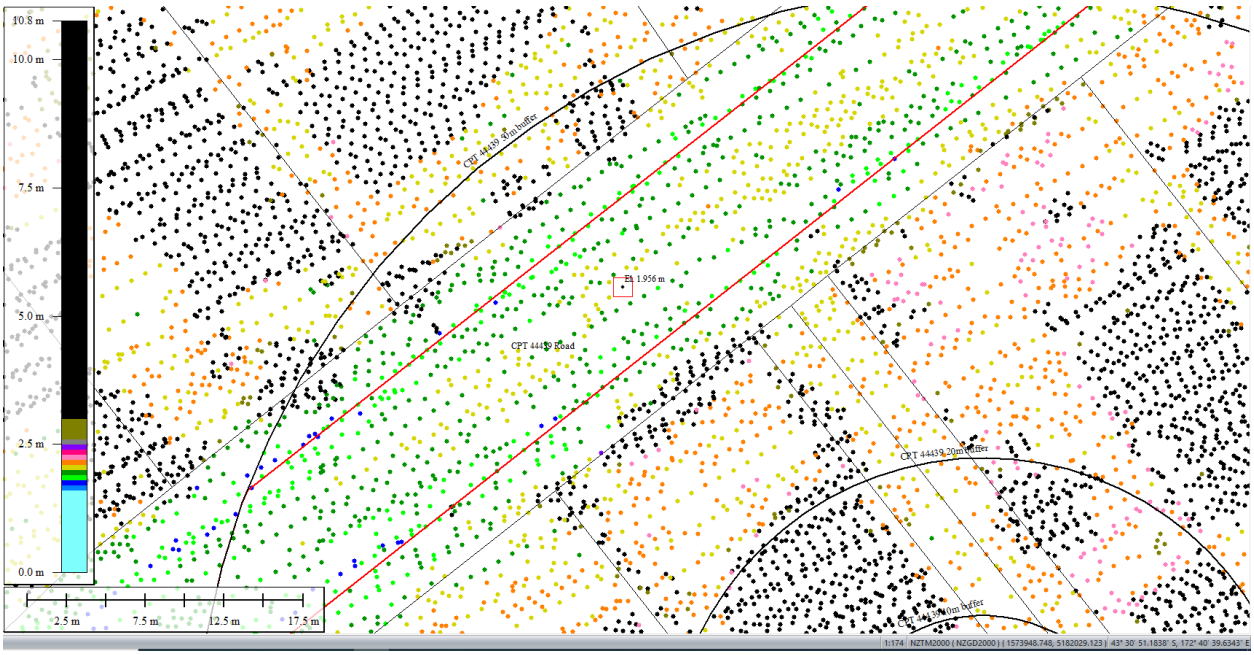

Figure 53: Ground surface elevation averaged over 50-m buffer for Road for Sep 5, 2010, LiDAR survey.

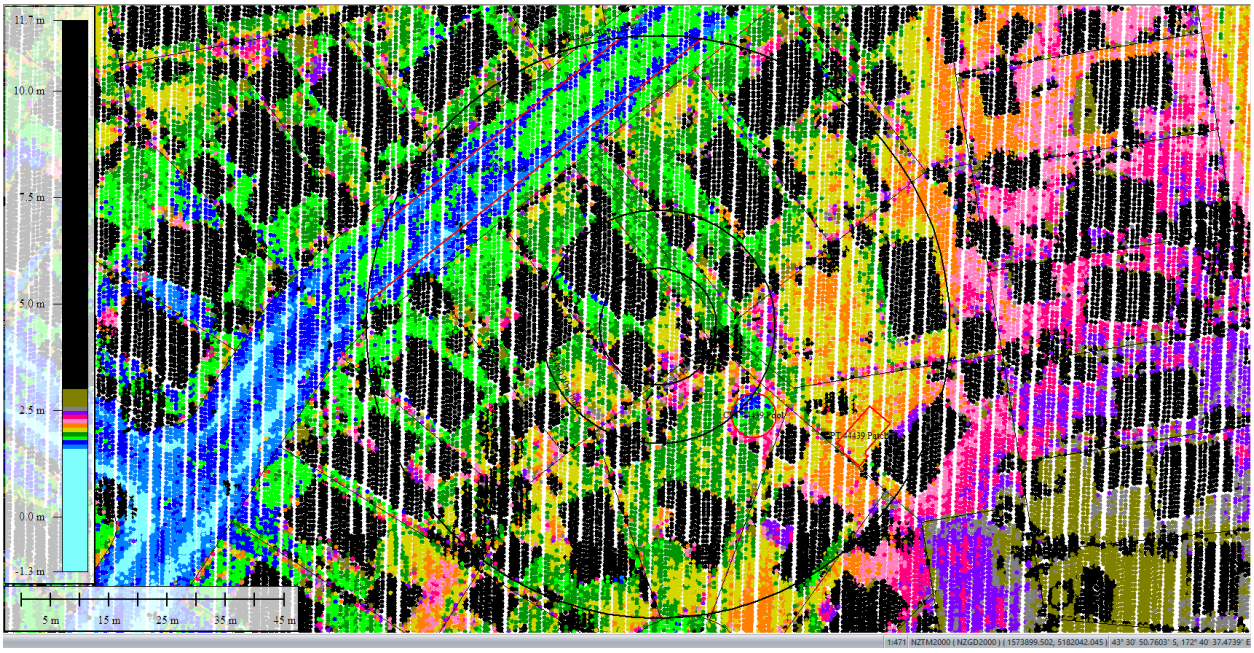

Figure 54: Mar 2011 LiDAR survey.

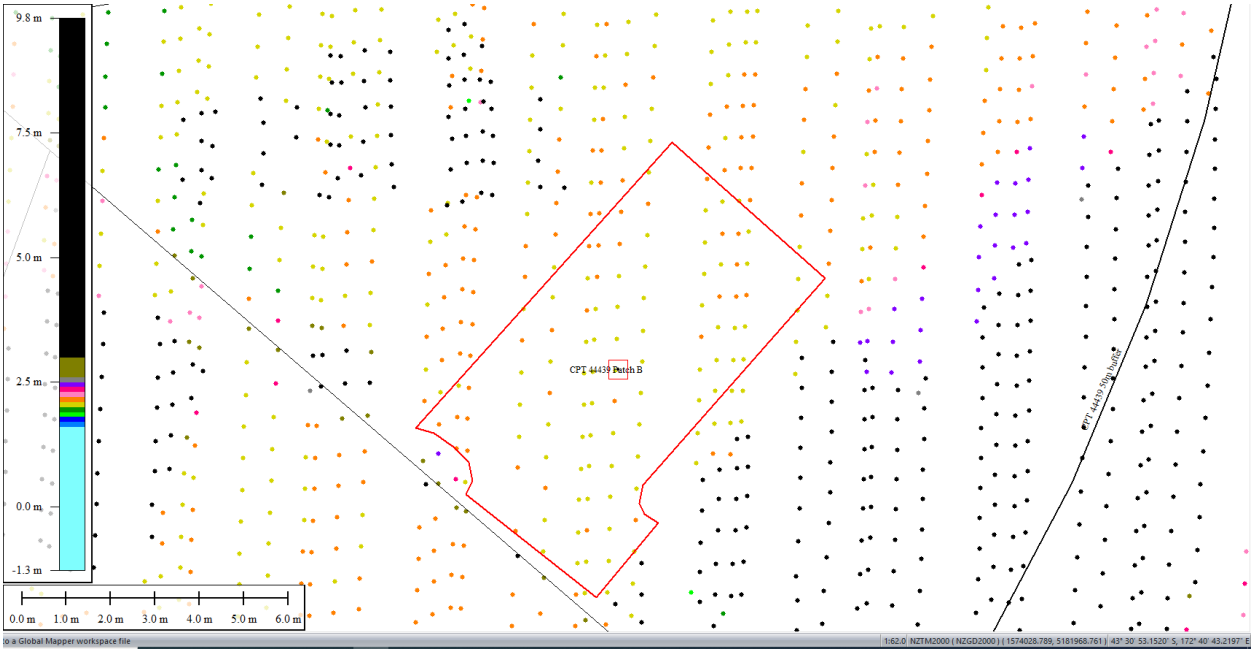

Figure 55: Ground surface elevation averaged over 50-m buffer for Patch B for Mar 2011 LiDAR survey (el. 2.091m).

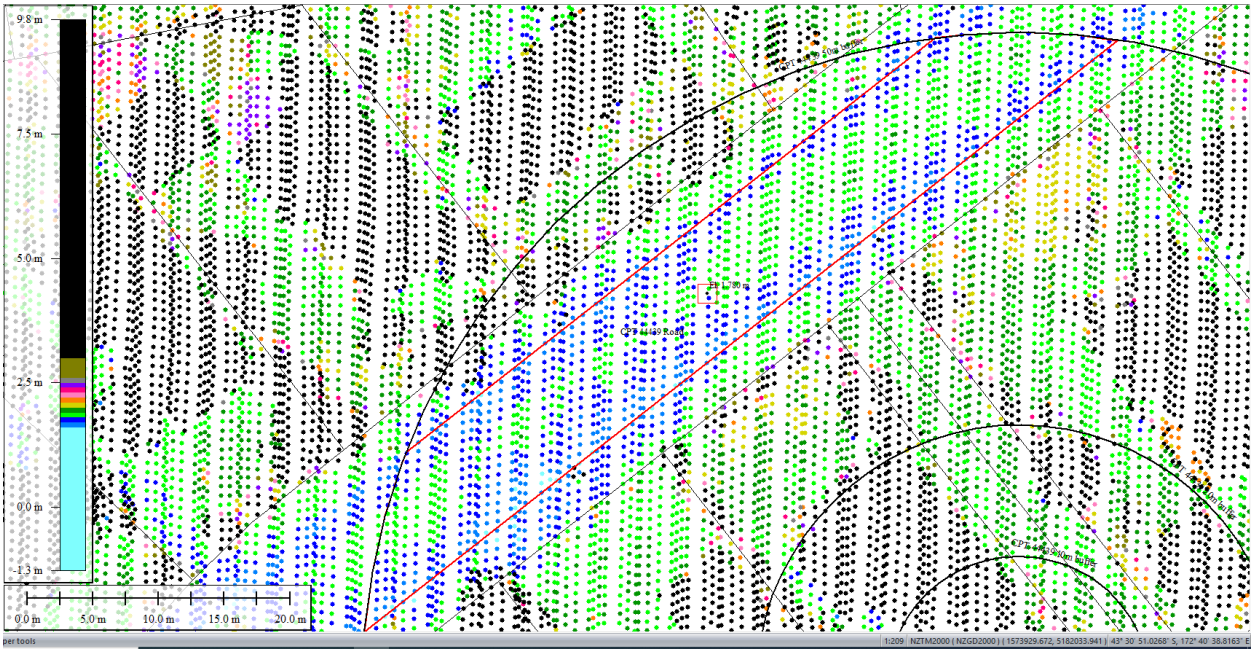

Figure 56: Ground surface elevation averaged over 50-m buffer for Road for Mar 2011 LiDAR survey.

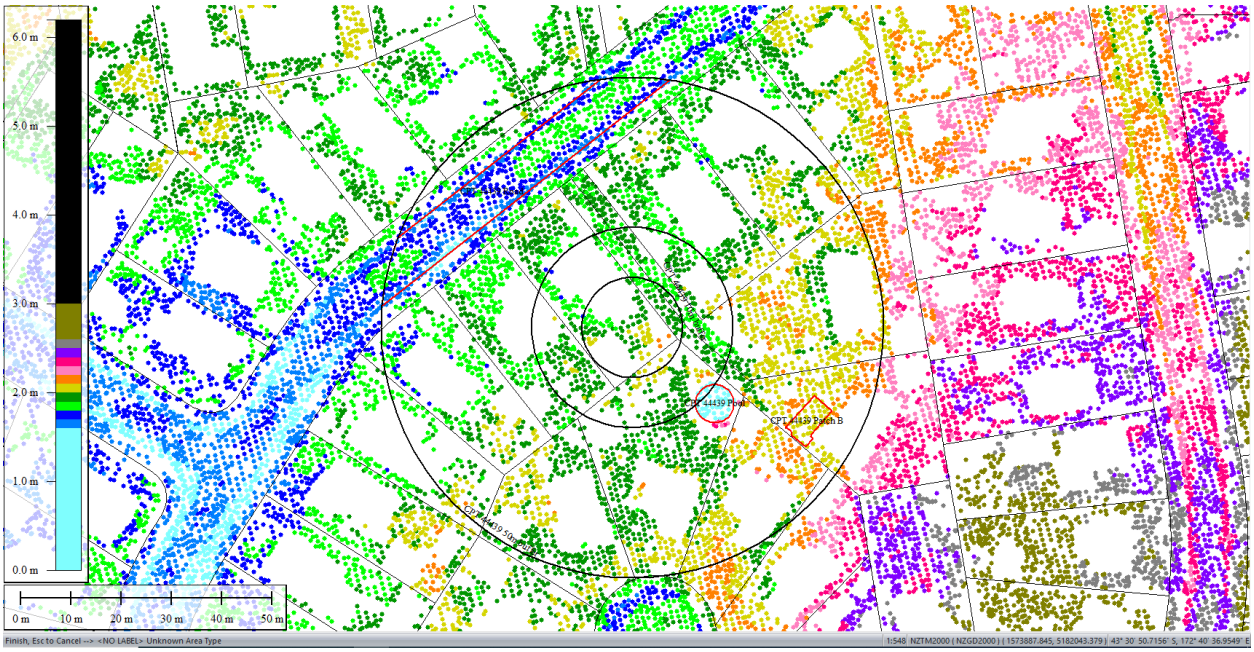

Figure 57: May 2011 LiDAR survey.

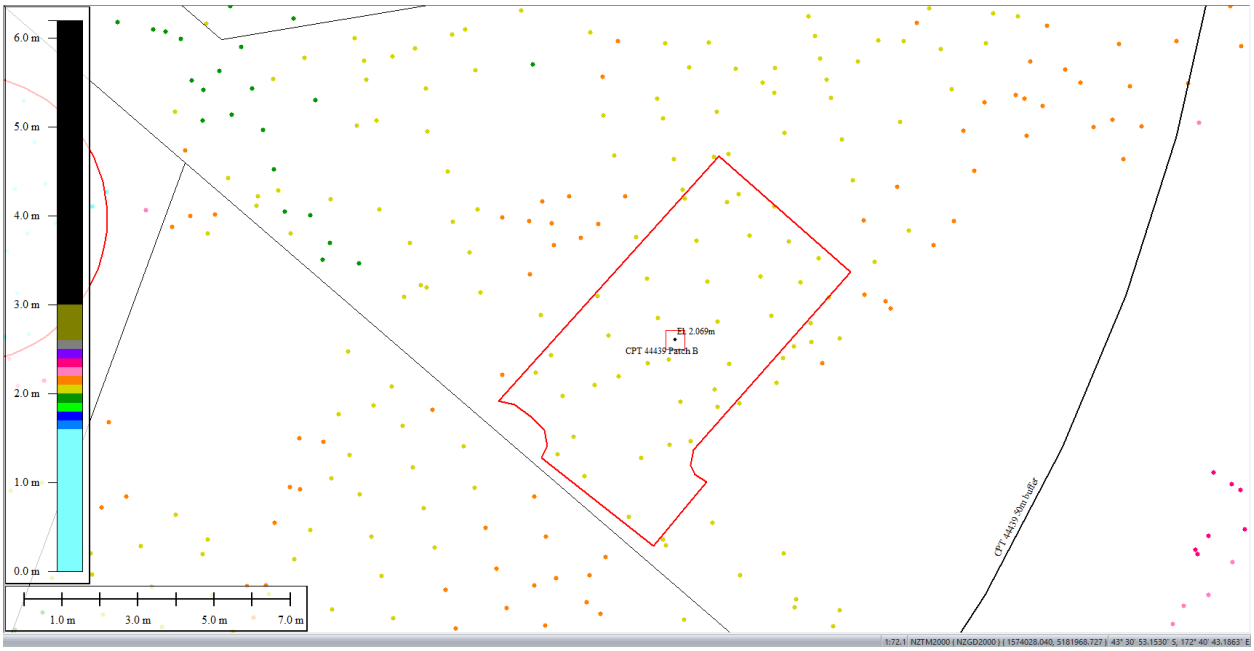

Figure 58: Ground surface elevation averaged over 50-m buffer for Patch B for May 2011 LiDAR survey.

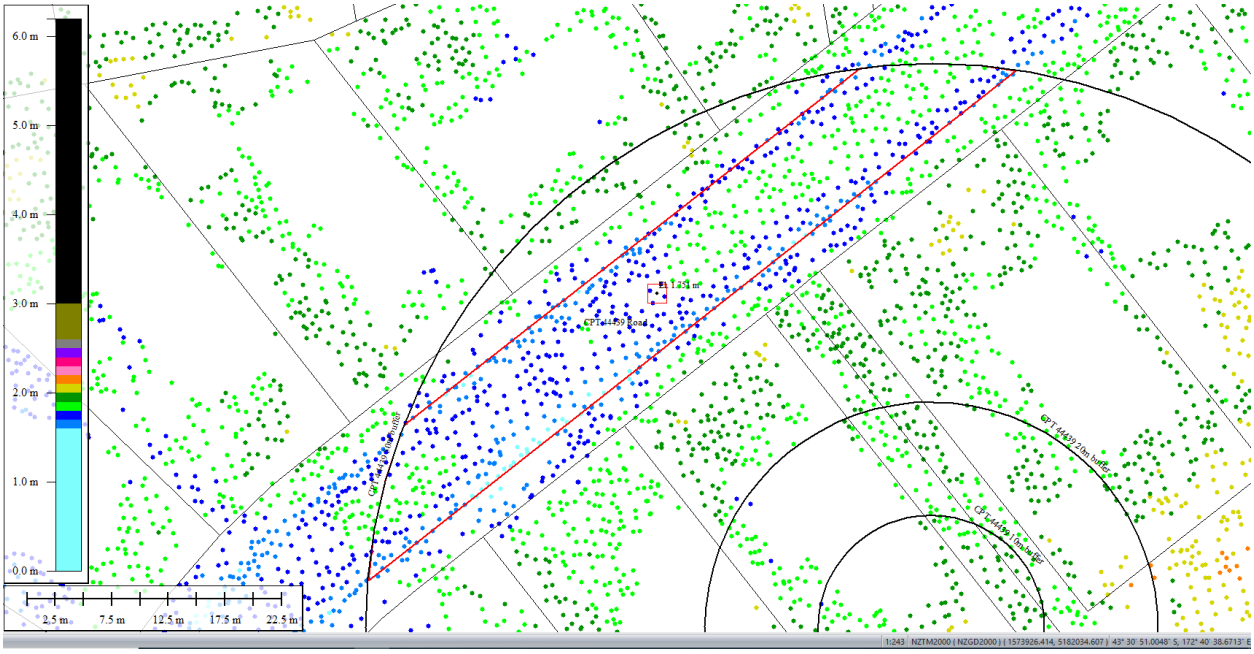

Figure 59: Ground surface elevation averaged over 50-m buffer for Road for May 2011 LiDAR survey.

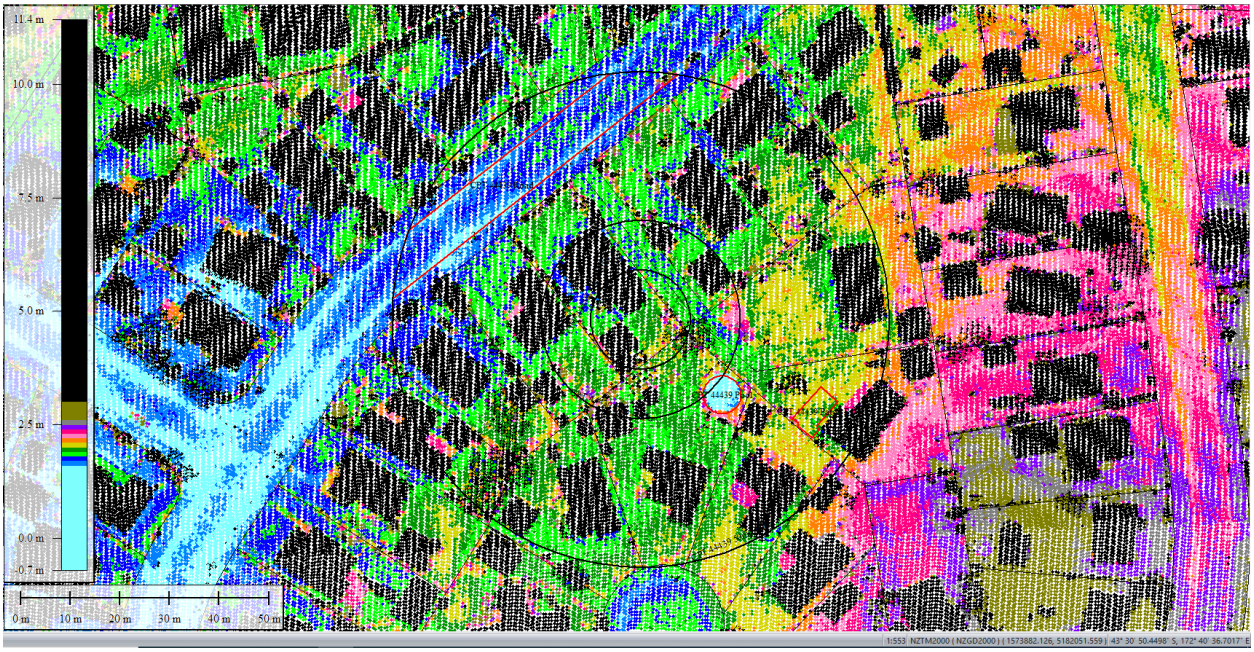

Figure 60: Sep 2011 LiDAR survey.

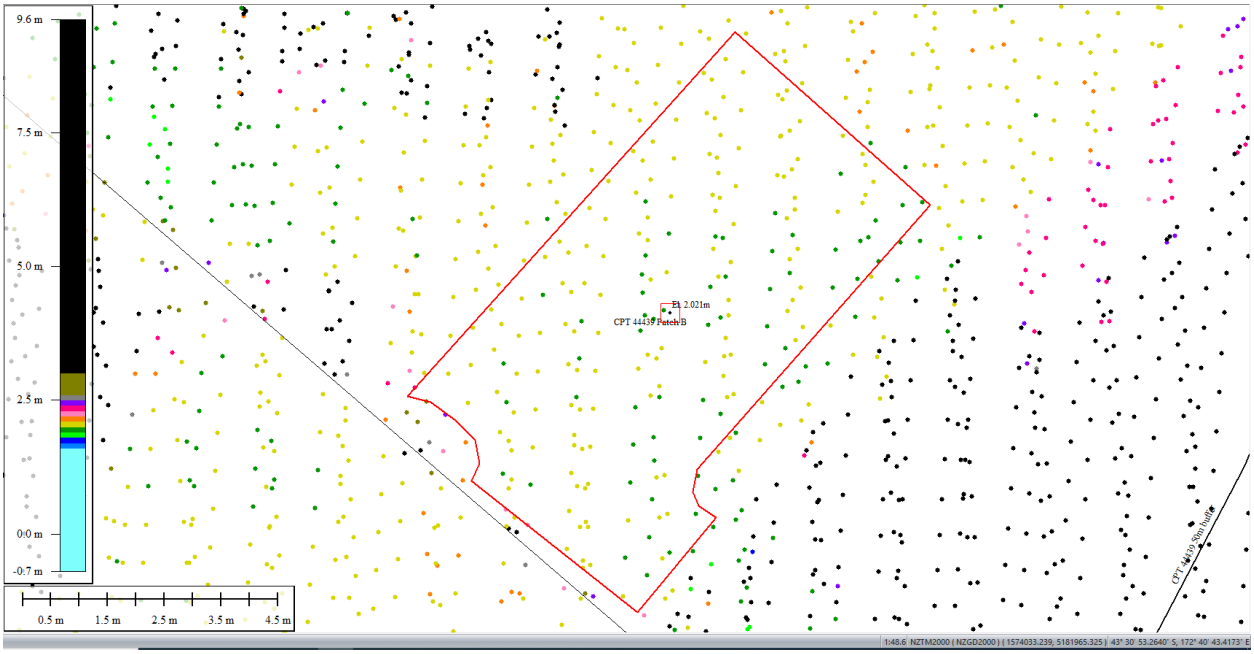

Figure 61: Ground surface elevation averaged over 50-m buffer for Patch B for Sep 2011 LiDAR survey.

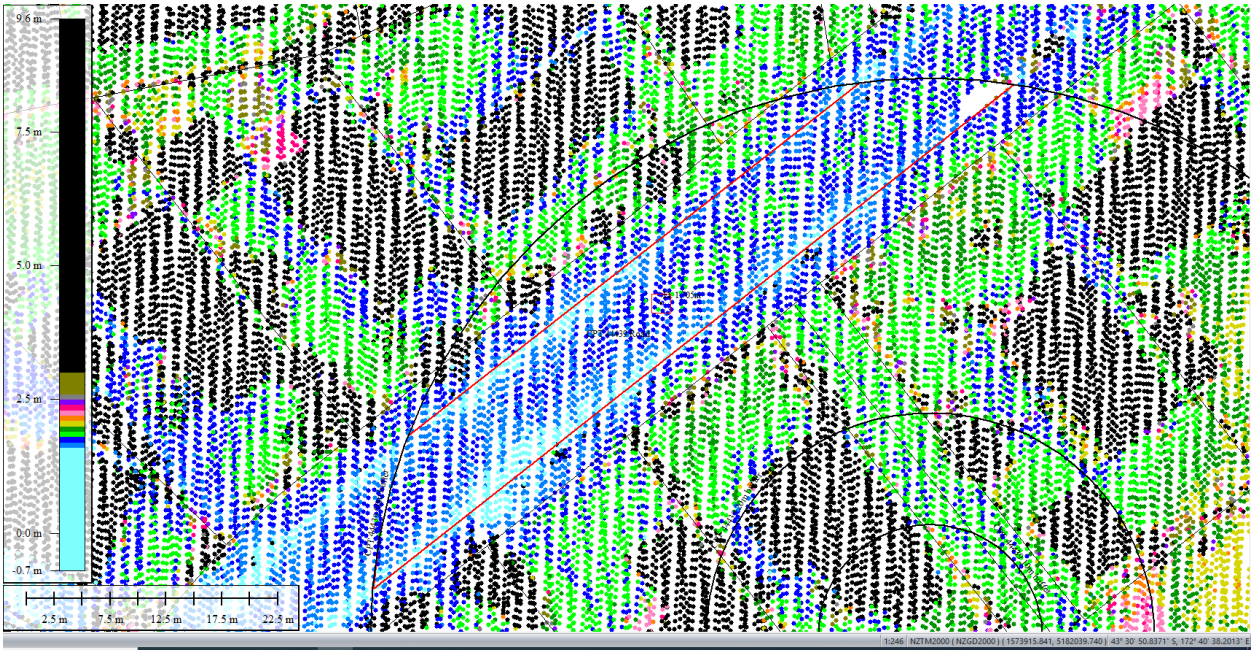

Figure 62: Ground surface elevation averaged over 50-m buffer for Road for Sep 2011 LiDAR survey.

Figure 63: Feb 2012 LiDAR survey.

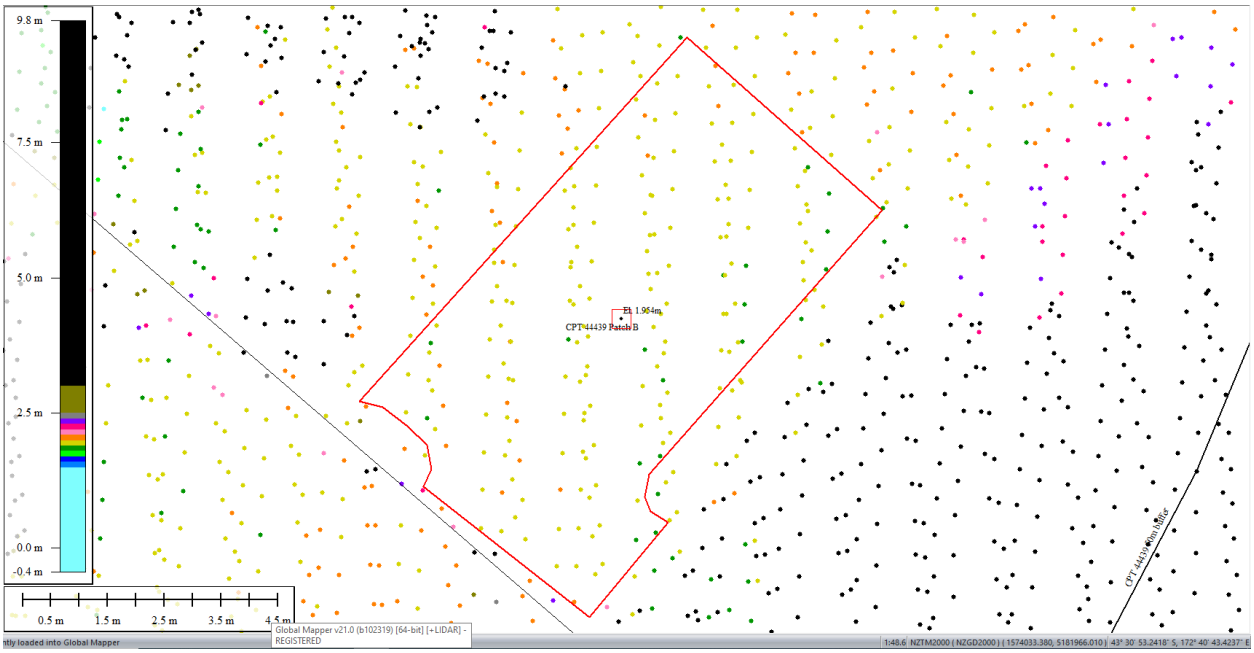

Figure 64: Ground surface elevation averaged over 50-m buffer for Patch B for Feb 2012 LiDAR survey.

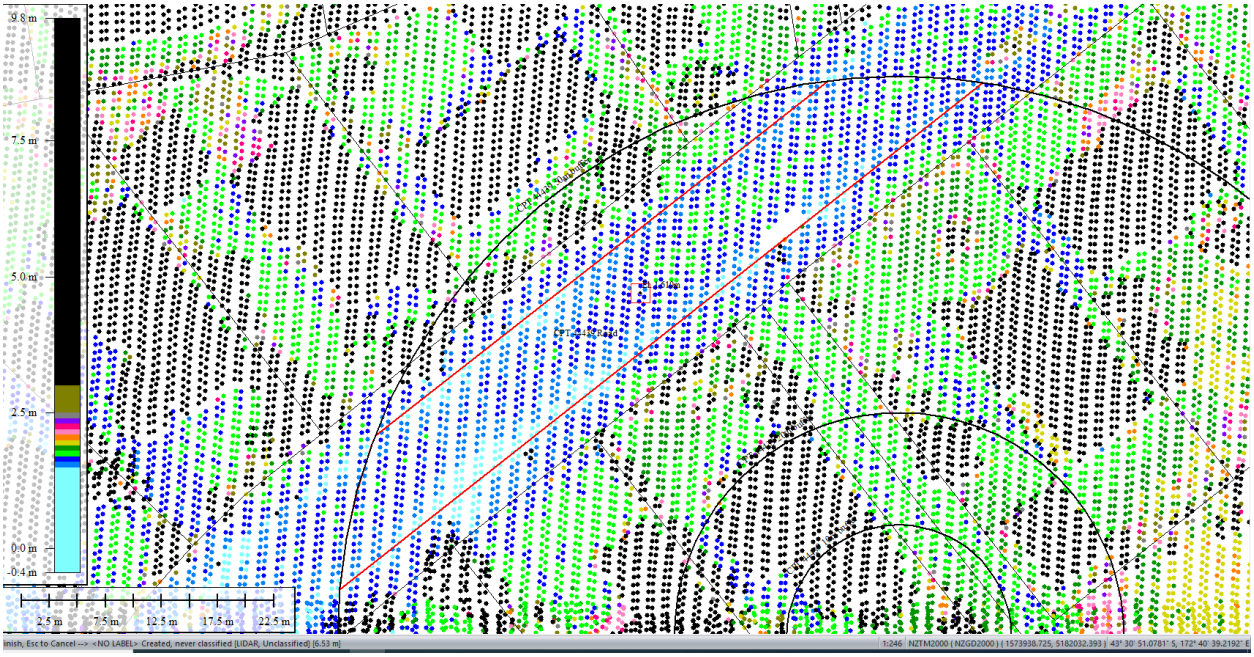

Figure 65: Ground surface elevation averaged over 50-m buffer for Road for Feb 2012 LiDAR survey.

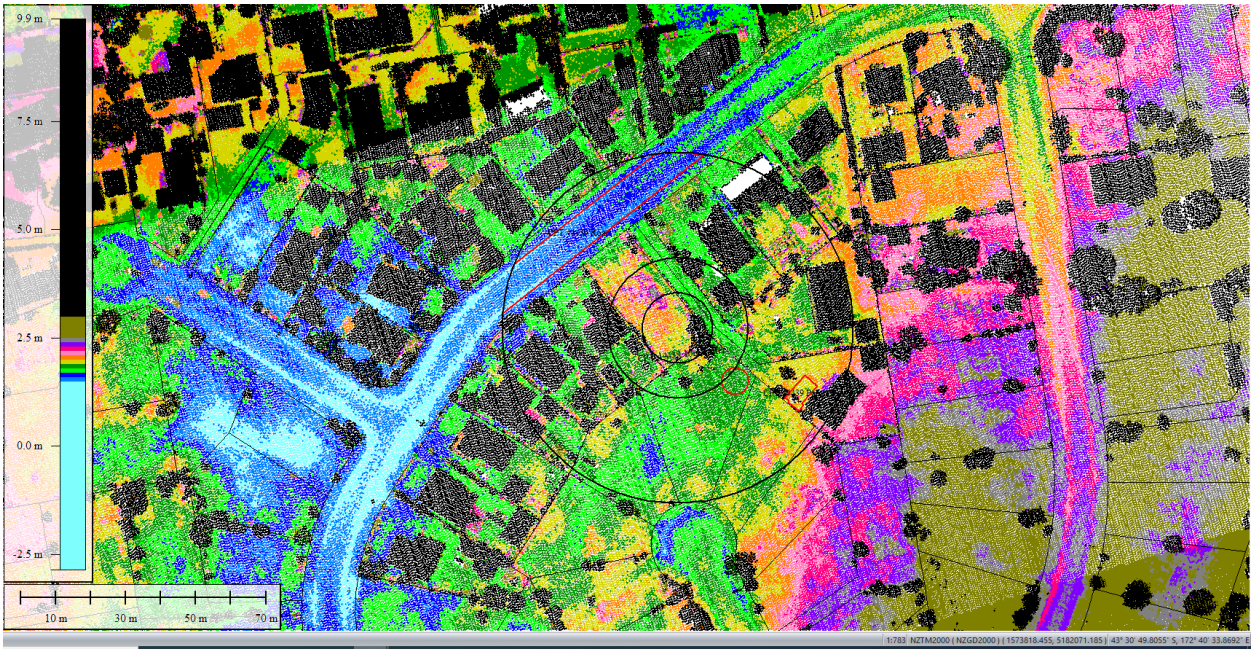

Figure 66: Oct 2015 LiDAR survey.

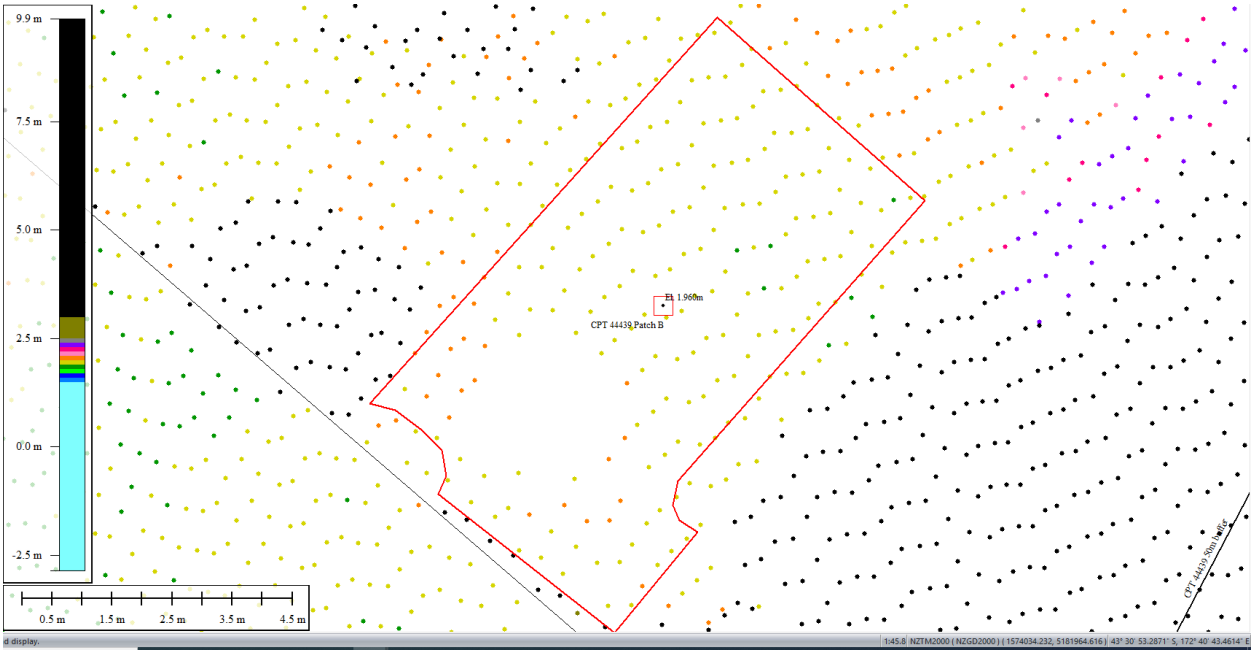

Figure 67: Ground surface elevation averaged over 50-m buffer for Patch B for Oct 2015 LiDAR survey.

Figure 68: Aerial photograph showing the ejecta outline at the site for the Sep-10 EQ.

Figure 69: Aerial photograph showing the ejecta outline at the site for the Feb-11 EQ.

Figure 70: Aerial photograph acquired on 16 Jun 2011 showing the ejecta outline at the site for the Jun-11 EQ.

Figure 71: Aerial photograph showing the ejecta outline at the site for the Dec-11 EQ.

Contents of this figure cannot be shared as doing so is restricted by a Non-Disclosure Agreement.

Figure 72: LDAT inspection notes for the property with Patch A (inspection date: 14 Oct 2010).

Contents of this figure cannot be shared as doing so is restricted by a Non-Disclosure Agreement.

Figure 73: LDAT inspection notes for the property with Patch A (inspection date: 17 June 2011).

Figure 74: Ground photographs showing ejecta at the property with Patch A (photograph date: 17 June 2011).

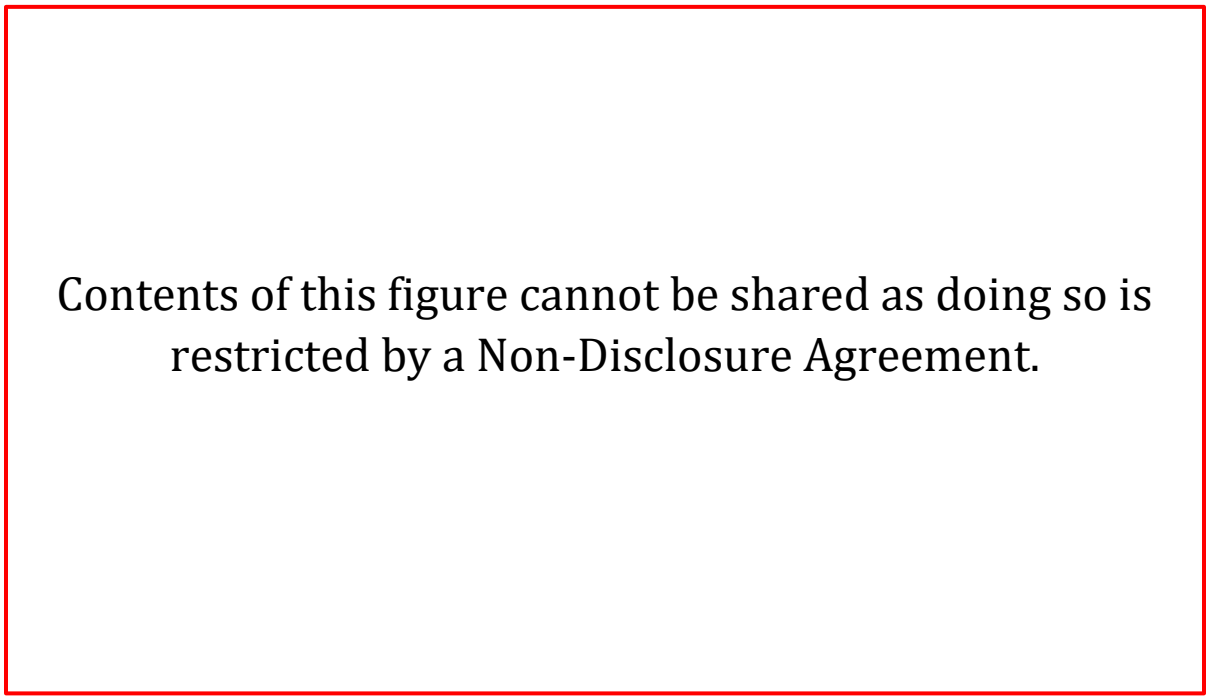

Figure 75: LDAT inspection notes for the property with Patch B (inspection date: 13 Oct 2010).

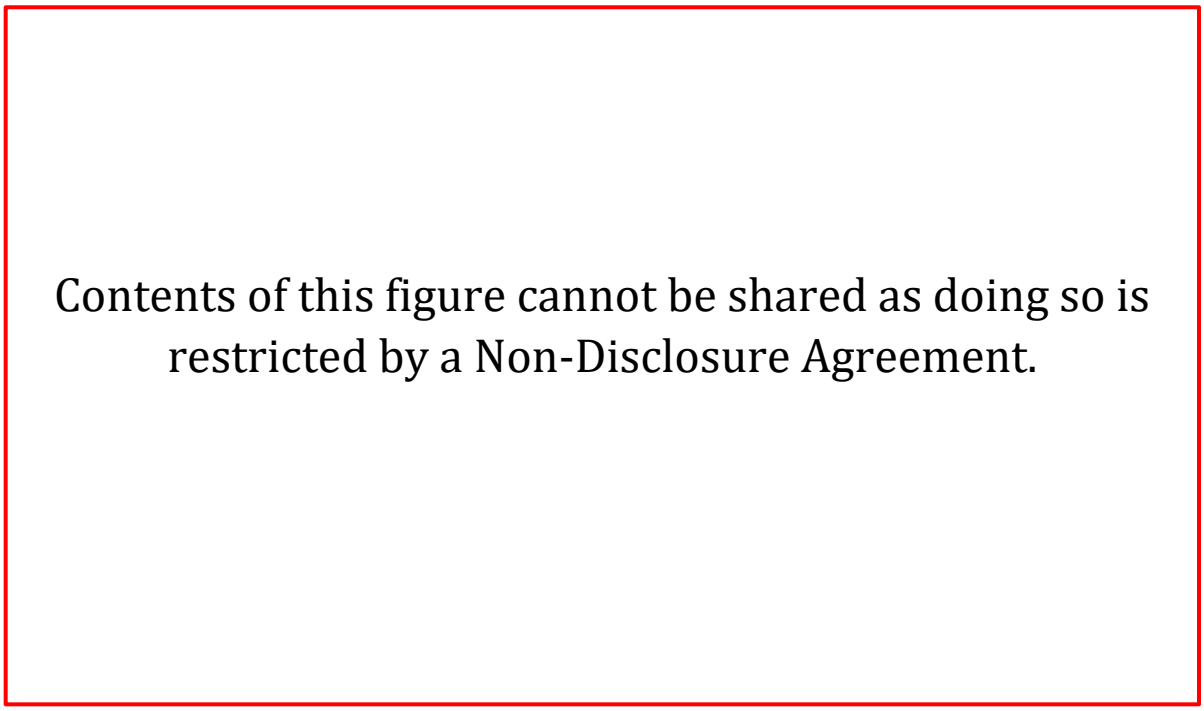

Figure 76: LDAT inspection notes for the property with Patch B (inspection date: 17 June 2011).

Figure 77: Ground photographs showing ejecta at the property with Patch B (photograph date: 13 Oct 2010).

Figure 78: Ground photographs showing ejecta at the property with Patch B (photograph date: 17 June 2011).

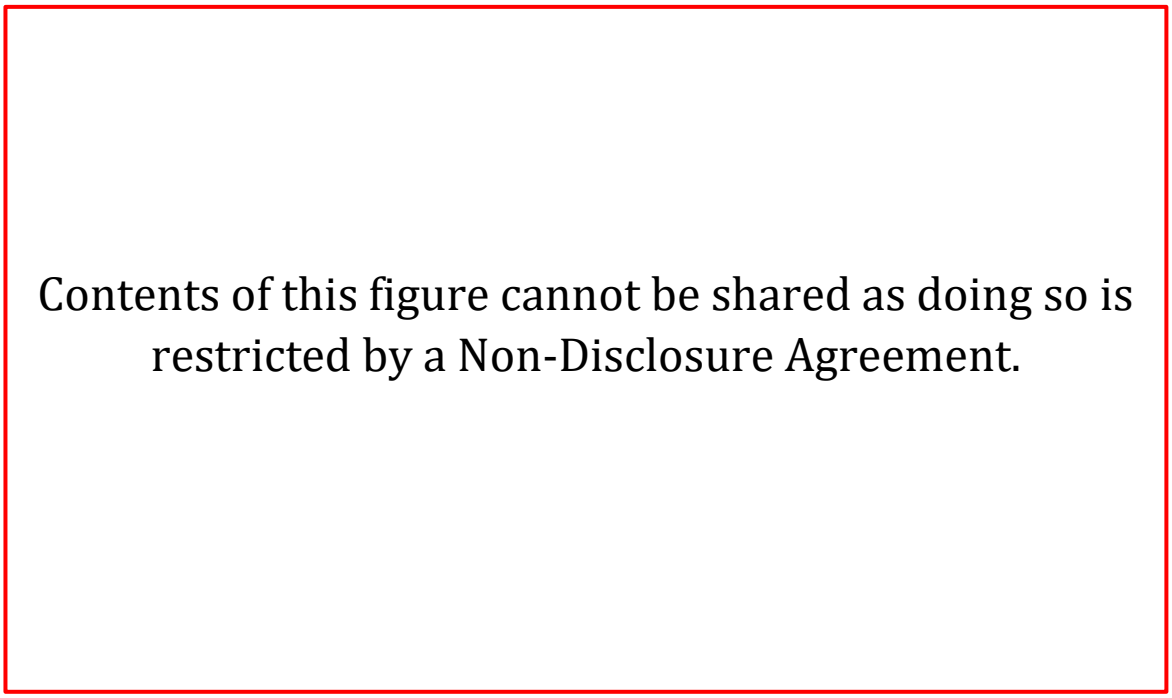

Figure 79: LDAT inspection notes for the property with Swimming Pool (inspection date: 13 Oct 2010).

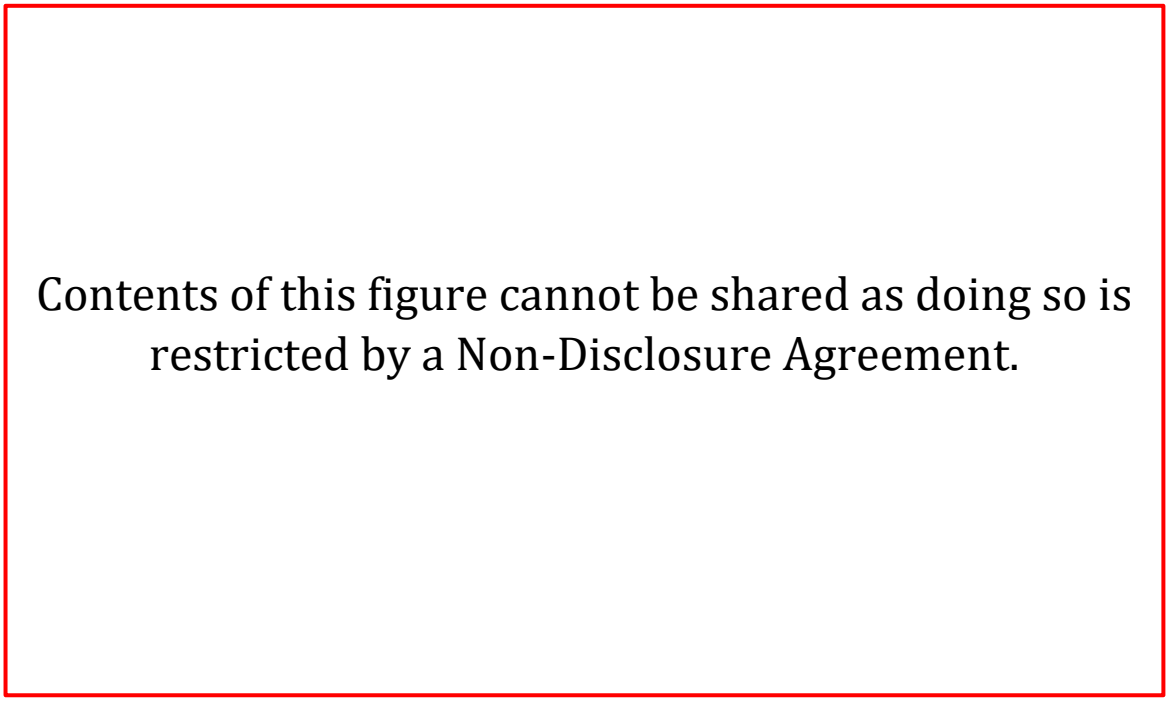

Figure 80: LDAT inspection notes for the property with Swimming Pool (inspection date: 17 June 2011).

Figure 81: Ground photographs showing ejecta in the Swimming Pool (photograph date: 17 June 2011).

Figure 82: Ground photographs showing ejecta at some properties within the 50-m buffer (photograph date: 17 June 2011).

Figure 83: PGA for Sep-10 EQ (st. dev. = 0.300-0.325 ln units).

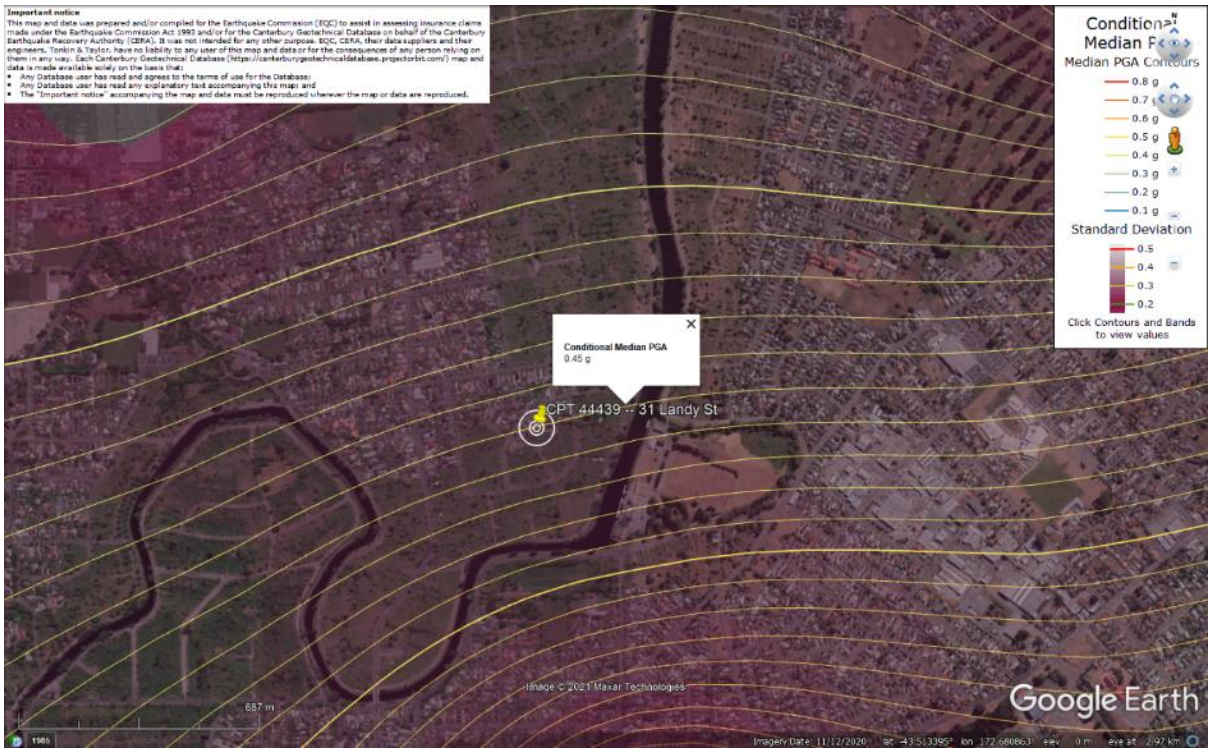

Figure 84: PGA for Feb-11 EQ (st. dev. = 0.300-0.325 ln units).

Figure 85: PGA for Jun-11 EQ (st. dev. = 0.325-0.350 ln units).

Figure 86: PGA for Dec-11 EQ (st. dev. = 0.375-0.400 ln units).

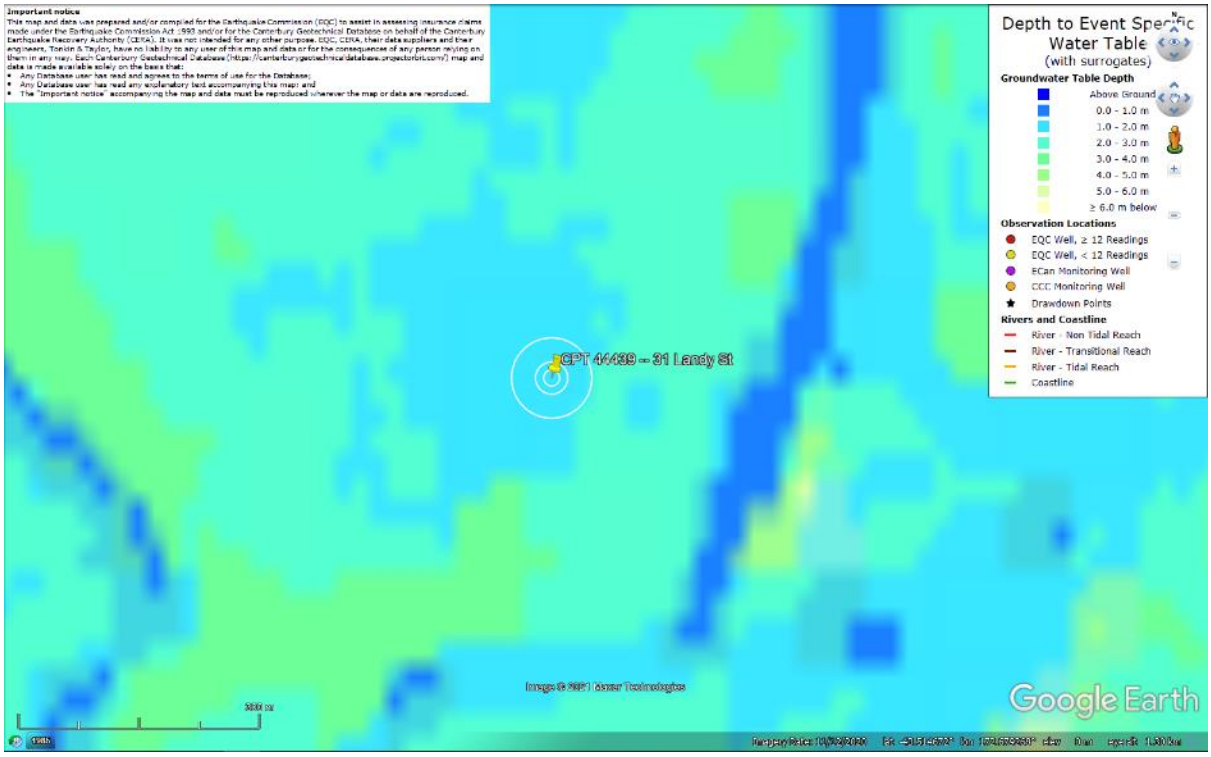

Figure 87: Depth to groundwater table for Sep-10 EQ.

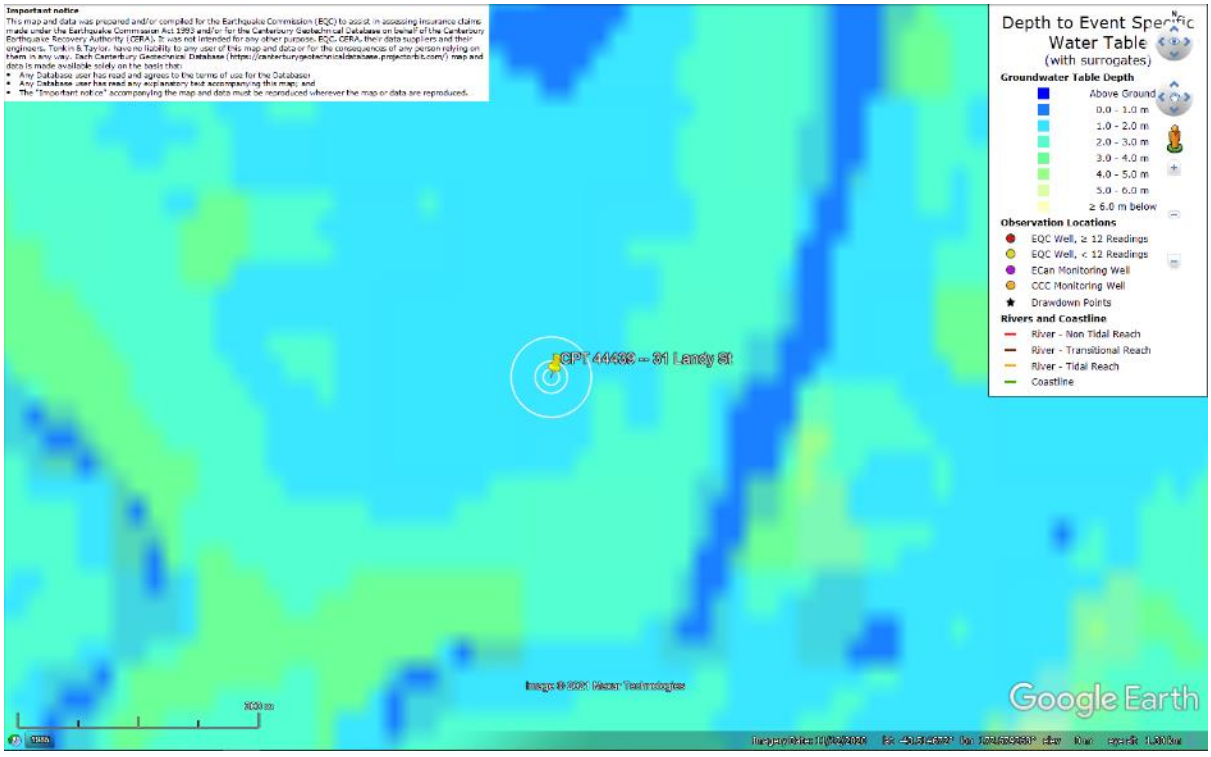

Figure 88: Depth to groundwater table for Feb-11 EQ.

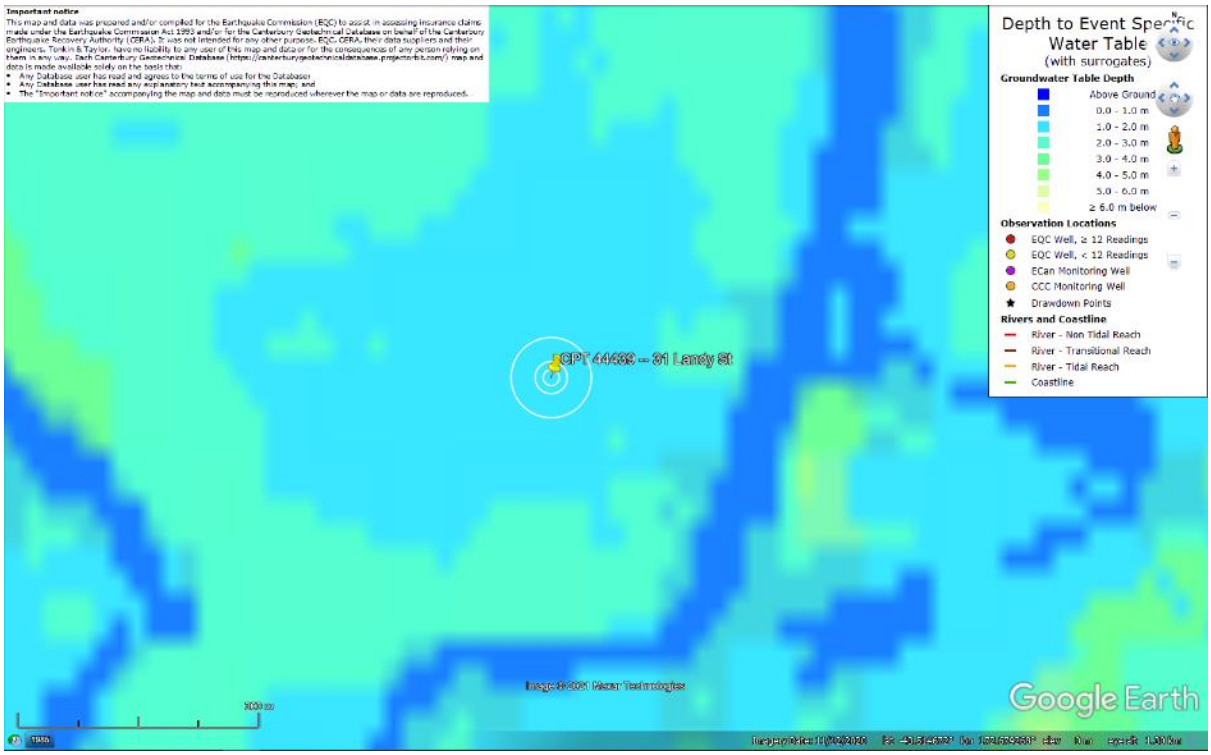

Figure 89: Depth to groundwater table for Jun-11 EQ.

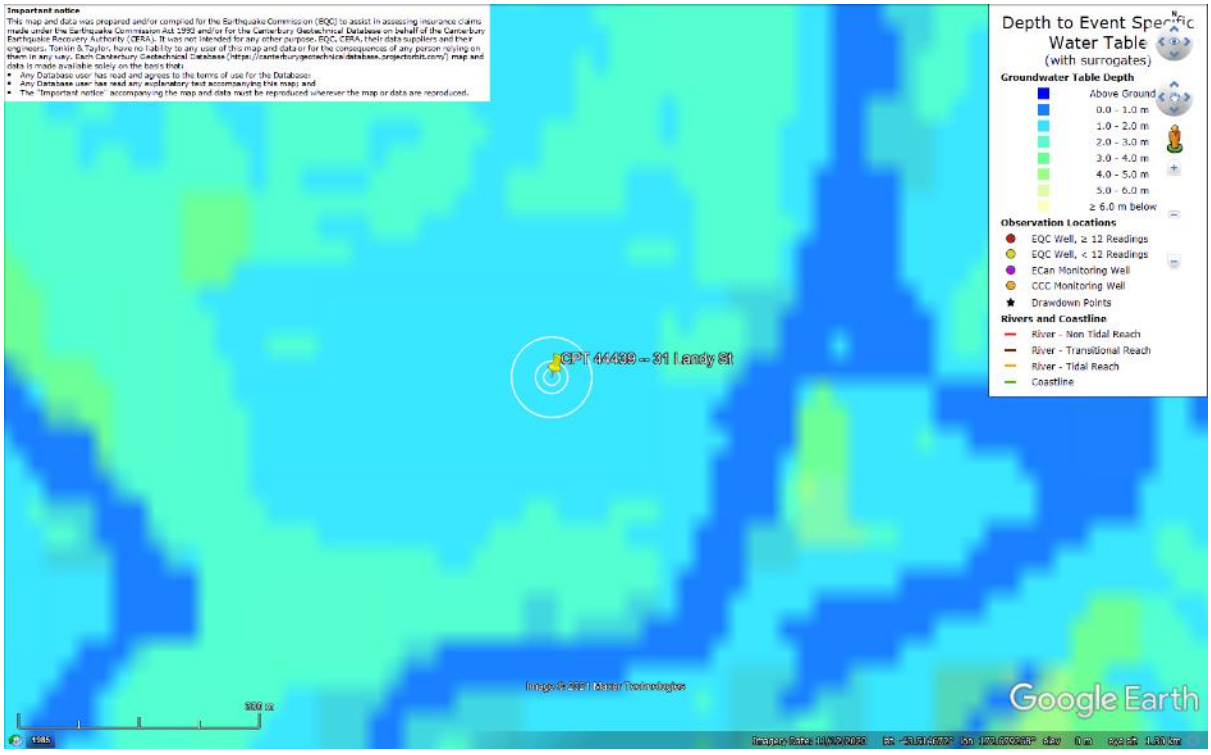

Figure 90: Depth to groundwater table for Dec-11 EQ.

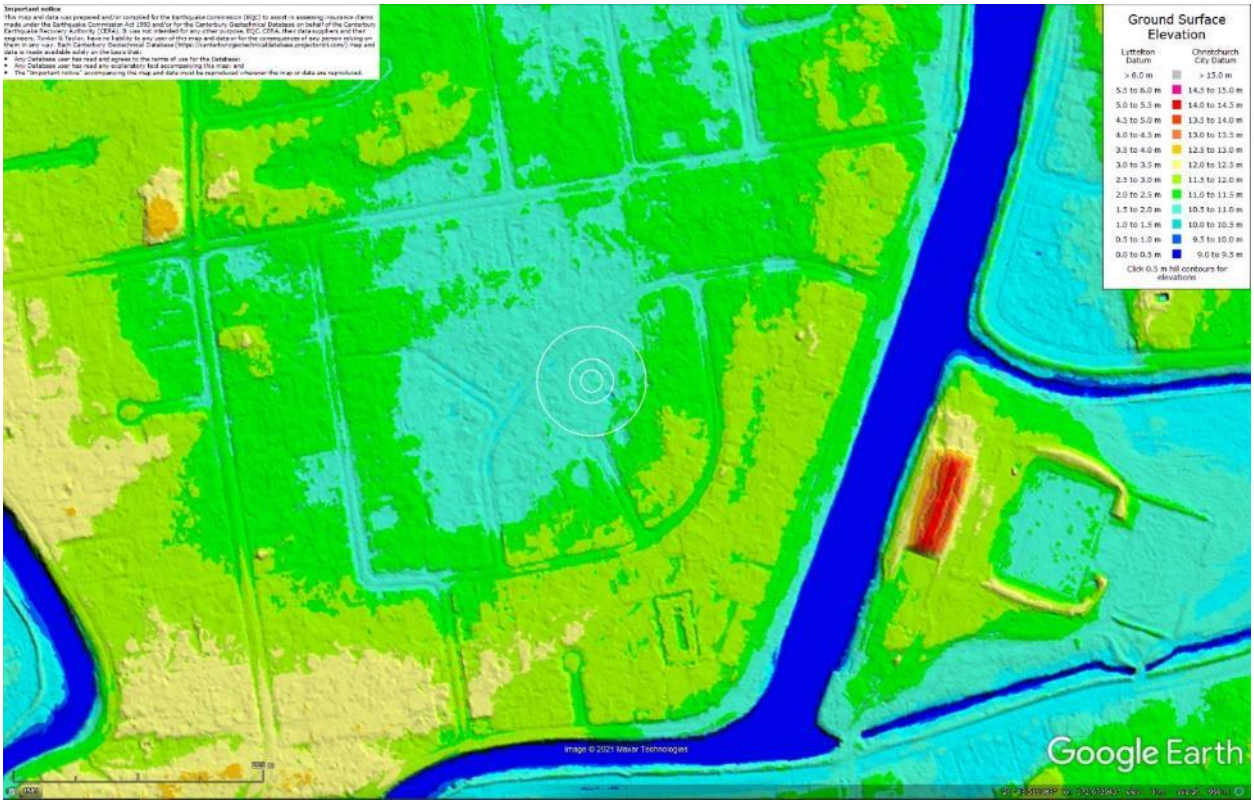

Figure 91: Ground surface elevation according to the Sep-11 LiDAR survey.

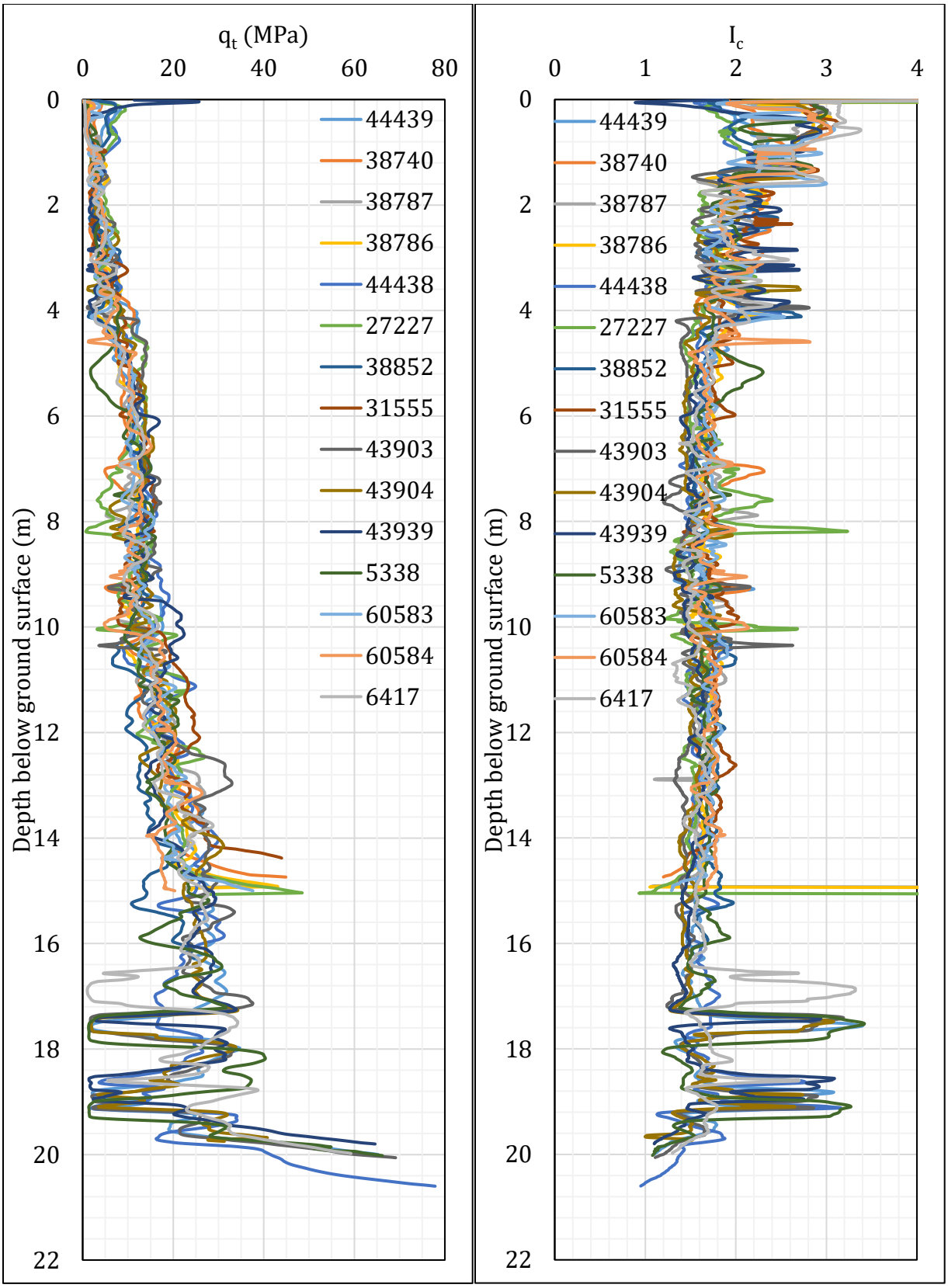

Figure 92: q_t and I_c profiles.

Note 6: The selection of CPTs for the area considered for settlement assessment (Figure 1) is based on the proximity of the CPTs to the considered areas. In accordance with that, the following table shows CPTs that were used for the volumetric settlement analysis in *Cliq v.3.0.3.2*, a CPT soil liquefaction software developed by GeoLogismiki. (The average volumetric settlements were reported in Table 8.)

Table 12: CPT profiles used in volumetric settlement analysis for areas selected for settlement assessment.

CPT ID No.	Patch A	Patch B	Swimming Pool	Road
44439	✓		✓	
38740				
38787				
38786				
44438				✓
27227		✓	✓	
38852				✓
31555				✓
43903				
43904				
43939				
5338				
60583				
60584				
6417				✓

Note: CPT 44439 was used to calculate the volumetric settlement for a depth range from ~15 m to 20 m for CPTs 38740, 38787, 38786, 60583, 60584, 27227, 31555, and 38852.

Table 13: CPT-based results.

		CPT ID							
EQ Event	Parameter	44439	38740	38787	38786	44438	27227	38852	31555
Sep-10	S_{V1D} (mm)	25	42	21	17	20	55	32	11
	LSN	6	10	4	3	5	10	6	3
	LPI	0	0	0	0	0	2	0	0
	LPI_{ish}	0	0	0	0	0	0	0	0
	$D_{FS<1}$ (m)	undet.	2.82	9.65	9.47	undet.	7.16	8.2	undet.
Feb-11	S_{V1D} (mm)	130	180	133	131	122	144	194	72
	LSN	33	40	33	31	31	34	39	21
	LPI	15	23	16	14	14	19	21	8
	LPI_{ish}	14	19	14	0	13	2	16	8
	$D_{FS<1}$ (m)	1.54	1.56	1.51	1.51	1.52	1.51	1.52	1.54
Jun-11	S_{V1D} (mm)	53	86	41	34	42	86	61	24
	LSN	16	22	10	7	13	20	13	7
	LPI	2	4	1	1	2	5	2	1
	LPI_{ish}	0	1	0	0	1	2	1	1
	$D_{FS<1}$ (m)	1.76	1.78	2.07	3.96	2.1	1.71	2.12	undet.
Dec-11	S_{V1D} (mm)	57	91	45	36	45	90	65	25
	LSN	17	24	11	8	14	21	14	8
	LPI	2	5	1	1	2	6	2	1
	LPI_{ish}	0	1	0	0	0	2	0	1
	$D_{FS<1}$ (m)	1.70	1.74	2.06	3.95	2.1	1.7	2.08	1.72

Notes: $D_{FS<1}$ = Depth to the first liquefiable layer ($FS_L<1$) that is at least 200-mm thick, as determined by the Boulanger and Idriss (2016) liquefaction-triggering procedure (P_L=50%, C_{FC}=0.13, and $I_{c,cutoff}$ =2.6), and exported from *Cliq v.3.0.3.2*; undet. = the specified soil layer was not detected.

Table 13 (continued): CPT-based results.

		CPT ID							
EQ Event	Parameter	43903	43904	43939	5338	60583	60584	6417	Δ_{CPT}
Sep-10	S_{V1D} (mm)	26	38	41	50	24	27	43	7
	LSN	7	8	10	10	6	5	8	0
	LPI	0	1	1	1	0	1	1	0
	LPI_{ish}	0	0	0	0	0	0	0	--
	$D_{FS<1}$ (m)	undet.	7.5	3.73	4.86	4.06	8.43	3.87	--
Feb-11	S_{V1D} (mm)	110	138	140	170	124	138	166	12
	LSN	29	33	35	39	31	34	36	1
	LPI	13	16	17	22	16	17	20	0
	LPI_{ish}	13	1	5	4	3	0	7	--
	$D_{FS<1}$ (m)	1.51	1.51	1.51	1.52	1.7	1.51	1.59	--
Jun-11	S_{V1D} (mm)	52	63	70	84	49	51	72	8
	LSN	16	15	20	20	13	11	16	0
	LPI	2	3	4	4	2	2	3	0
	LPI_{ish}	1	1	2	1	1	1	1	--
	$D_{FS<1}$ (m)	1.51	1.98	1.73	2.26	2.26	3.02	2.86	--
Dec-11	S_{V1D} (mm)	55	65	74	89	52	54	76	8
	LSN	17	16	21	21	14	12	17	0
	LPI	3	3	5	5	3	2	4	0
	LPI_{ish}	1	1	2	1	0	0	0	--
	$D_{FS<1}$ (m)	1.51	2.91	1.71	1.96	3.15	2.99	2.86	--

Notes: $D_{FS<1}$ = Depth to the first liquefiable layer ($FS_L<1$) that is at least 200-mm thick, as determined by the Boulanger and Idriss (2016) liquefaction-triggering procedure (P_L=50%, C_{FC}=0.13, and $I_{c,cutoff}$ =2.6), and exported from *Cliq v.3.0.3.2*; undet. = the specified soil layer was not detected; Δ_{CPT} indicates the amount of SV1D, LSN, and LPI added for CPTs 38740, 38787, 38786, 60583, 60584, 27227, 31555, and 38852 due to the penetration depths shallower than 20 m.

Note 7: Based on the borehole log (BH 16249, Figure 1), the groundwater table is at a depth of 1.95 m below the ground surface. The soil profile consists of (1) gravelly, GW, fill below asphalt to a depth of 0.3 m, (2) sandy silt, ML, the Yaldhurst member of the Springston formation to a depth of 2 m, (3) fine to medium sand, SP, of the Christchurch formation, to a depth of 8 m, (4) gravelly fine to coarse sand, SW, of the Christchurch formation, to a depth of 8.9 m, and (5) fine to medium sand, SP, of the Christchurch formation, to a depth of 20 m.

Note 8: The ejecta-induced free-field settlement provided in Table 11 is an areal average settlement due to ejecta, which is based on the total settlement assessment area, A_T (provided in Table 9 and repeated in Table 14). However, the considered area was not always covered completely with ejecta; thus, it is important to provide the localized ejecta-induced settlement, too. The localized settlement due to ejecta is estimated using photographic evidence only as

$$S_{E,P\_localized} = \frac{V_E}{A_E}$$

where V_E is the total volume of ejecta within A_T and A_E is the total coverage area of ejecta within A_T. Please note that the areal ejecta-induced settlement provided in Table 14 as S_{E,P_areal} is the same as $S_{E,P}$ in Table 11, which was estimated as

$$S_{E,P\_areal} = S_{E,P} = \frac{V_E}{A_T}$$

where V_E is the total volume of ejecta within A_T and A_T is the total settlement assessment area.

Table 14a: Areal and localized ejecta-induced settlement estimates for Patch B (50-m buffer) based on photographic evidence.

Earthquake Event	A_T (m^2)	A_E (m^2)	V_E (m^3)	S_{E,P_areal} (mm)	$S_{E,P\_localized}$ (mm)
Sep-10	42.4	42.4	0.9-2.2	35±15	35±15
Feb-11	42.1	42.1	1.7-2.6	50±10	50±10
Jun-11	22.9	15.2	0.4-0.9	30±10	45±15
Dec-11	42.4	0	0	0	0

Notes: S_{E,P_areal} = $S_{E,P}$ reported in Table 11 = areal ejecta-induced settlement; $S_{E,P\_localized}$ = localized ejecta-induced settlement; A_T = total settlement assessment area; V_E = total volume of ejecta within A_T; A_E = total area of ejecta within A_T; The estimates of both areal and localized ejecta-induced settlement are rounded to the nearest 5; Final plus/minus values are also rounded to the nearest 5.

Table 14b: Areal and localized ejecta-induced settlement estimates for Road (50-m buffer) based on photographic evidence.

Earthquake Event	A_T (m^2)	A_E (m^2)	V_E (m^3)	S_{E,P_areal} (mm)	$S_{E,P\_localized}$ (mm)
Sep-10	565	540	11.6-17.8	25±5	30±5
Feb-11	562	562	22.5-35.8	50±10	50±10
Jun-11	478	478	15.2-24.8	40±10	40±10
Dec-11	563	203	4.8-6.3	10±5	30±5

Notes: S_{E,P_areal} = $S_{E,P}$ reported in Table 11 = areal ejecta-induced settlement; $S_{E,P\_localized}$ = localized ejecta-induced settlement; A_T = total settlement assessment area; V_E = total volume of ejecta within A_T; A_E = total area of ejecta within A_T; The estimates of both areal and localized ejecta-induced settlement are rounded to the nearest 5; Final plus/minus values are also rounded to the nearest 5.

Summary 2:

- **The best estimate of the localized ejecta-induced free-field ground settlement at the 31 Landy St site for the SEP 2010, FEB 2011, JUN 2011, and DEC 2011 earthquake is 35±15 mm, 50±10 mm, 45±15 mm, and 0 mm, respectively.**
- **The best estimate of the localized ejecta-induced settlement of the road at the 31 Landy St site for the SEP 2010, FEB 2011, JUN 2011, and DEC 2011 earthquake is 30±5 mm, 50±10 mm, 40±10 mm, and 30±5 mm, respectively.**